A Continuation BSOR-Lanczos-Galerkin Method for Positive Bound States of A Multi-Component Bose-Einstein Condensate

Shu-Ming Chang, Yuen-Cheng Kuo, Wen-Wei Lin, Shih-Feng Shieh

Department of Mathematics, National Tsing Hua University, Hsinchu, Taiwan

Abstract

We develop a continuation block successive over-relaxation (BSOR)-Lanczos-Galerkin method for the computation of positive bound states of time-independent, coupled Gross-Pitaevskii equations (CGPEs) which describe a multi-component Bose-Einstein condensate (BEC). A discretization of the CGPEs leads to a nonlinear algebraic eigenvalue problem (NAEP). The solution curve with respect to some parameter of the NAEP is then followed by the proposed method. For a single-component BEC, we prove that there exists a unique global minimizer (the ground state) which is represented by an ordinary differential equation with the initial value. For a multi-component BEC, we prove that m identical ground/bound states will bifurcate into m different ground/bound states at a finite repulsive inter-component scattering length. Numerical results show that various positive bound states of a two/three-component BEC are solved efficiently and reliably by the continuation BSOR-Lanczos-Galerkin method.

Key words: Multi-Component Bose-Einstein Condensate, Continuation BSOR-Lanczos-Galerkin Method, Gross-Pitaevskii equation, Gauss-Seidel-type iteration, Nonlinear Schrödinger equation

1 Introduction

In this paper, we mainly propose a continuation block successive over-relaxation (BSOR)-Lanczos-Galerkin method for the computation of positive bound states

Email addresses: m863254@am.nthu.edu.tw (Shu-Ming Chang), m883207@am.nthu.edu.tw (Yuen-Cheng Kuo), wwlin@am.nthu.edu.tw (Wen-Wei Lin), sfshieh@am.nthu.edu.tw (Shih-Feng Shieh).

of a multi-component Bose-Einstein Condensate (BEC). It is well-known (4; 26; 29) that coupled Gross-Pitaevskii equations (CGPEs), also called coupled nonlinear Schrödinger equations,

$$\boldsymbol{\iota}\frac{\partial\psi_j(\mathbf{x},t)}{\partial t} = -\nabla^2\psi_j + V_j(\mathbf{x})\psi_j + \alpha_j|\psi_j|^2\psi_j + \sum_{k\neq j}\beta_{kj}|\psi_k|^2\psi_j, \tag{1.1a}$$

$$\mathbf{x}\in\Omega\subseteq\mathbb{R}^2 \text{ or } \mathbb{R}^3,\ t>0,\ \boldsymbol{\iota}=\sqrt{-1}, \tag{1.1b}$$

$$\psi_j(\mathbf{x},t)=0,\ \mathbf{x}\in\partial\Omega,\ j=1,\ldots,m, \tag{1.1c}$$

can be used as a mathematical model to describe a multi-component BEC in m different hyperfine spin states on the corresponding condensate wave functions ψ_j's. Here Ω is a bounded smooth domain, $V_j(\mathbf{x})\geq 0$, $j=1,\ldots,m$ are magnetic trapping potentials, and the nonnegative constants α_j's and $\beta_{kj}=\beta_{jk}$'s, $k\neq j$, $k,j=1,\ldots,m$ are the intra-component and inter-component (repulsive) scattering lengths, respectively, which represent the interactions between like and unlike particles. In fact, for simplicity, here we choose suitable scales for Planck constant, atom mass and mean number of atoms in hyperfine states to make the CGPEs (1.1) consistent with the physical model (4). Furthermore, CGPEs (1.1) conserve the normalization of each component, i.e.

$$\int_\Omega|\psi_j(\mathbf{x},t)|^2d\mathbf{x}=1,\ j=1,\ldots,m. \tag{1.2}$$

To find solitary wave solutions of the system (1.1), we set

$$\psi_j(\mathbf{x},t)=e^{-\boldsymbol{\iota}\lambda_j t}\phi_j(\mathbf{x}),\ j=1,\ldots,m. \tag{1.3}$$

Plugging (1.3) into (1.1a) and using (1.2) gives a nonlinear eigenvalue problem (NEP), also called time-independent CGPEs or Hatree-Fock equations (19; 20),

$$-\nabla^2\phi_j + V_j\phi_j + \alpha_j|\phi_j|^2\phi_j + \sum_{k\neq j}\beta_{kj}|\phi_k|^2\phi_j = \lambda_j\phi_j,\ \text{in } \Omega, \tag{1.4a}$$

$$\int_\Omega|\phi_j(\mathbf{x})|^2d\mathbf{x}=1,\ j=1,\ldots,m. \tag{1.4b}$$

To investigate ground state solutions of a multi-component BEC, (4) shows that the ground states can be found by minimizing the energy functional $E(\boldsymbol{\phi})$ with $\boldsymbol{\phi}=(\phi_1,\ldots,\phi_m)$ under conditions (1.4b), i.e.,

$$\begin{aligned}&\underset{\boldsymbol{\phi}=(\phi_1,\ldots,\phi_m)}{\text{Minimize}}\ E(\boldsymbol{\phi})\\ &\text{subject to}\ \int_\Omega|\phi_j(\mathbf{x})|^2d\mathbf{x}=1,\ \phi_j(\mathbf{x})>0,\ j=1,\ldots,m,\end{aligned} \tag{1.5a}$$

where

$$E(\boldsymbol{\phi}) = \sum_{j=1}^{m} \int_{\Omega} \left(\frac{1}{2} |\nabla \phi_j|^2 + \frac{1}{2} V_j |\phi_j|^2 + \frac{\alpha_j}{4} |\phi_j|^4 \right) + \frac{1}{4} \sum_{k,j=1, k \neq j}^{m} \beta_{kj} \int_{\Omega} |\phi_k|^2 |\phi_j|^2. \tag{1.5b}$$

On the other hand, equations (1.4) can also be regarded as Euler-Lagrange equations of the optimization problem (1.5). Furthermore, multiplying the j-th equation in (1.4a) by $\phi_j(\mathbf{x})$, and using (1.4b) and (1.5b) it is easily seen that any eigenvalue vector $\boldsymbol{\lambda} = (\lambda_1, \ldots, \lambda_m)$ and the corresponding eigenfunction vector $\boldsymbol{\phi} = (\phi_1, \ldots, \phi_m)$ of (1.4) satisfy

$$\sum_{j=1}^{m} \lambda_j = 2E(\boldsymbol{\phi}) + \frac{1}{2} \sum_{k,j=1, k \neq j}^{m} \beta_{kj} \int_{\Omega} |\phi_k|^2 |\phi_j|^2 + \frac{1}{2} \sum_{j=1}^{m} \alpha_j \int_{\Omega} |\phi_j|^4. \tag{1.6}$$

In ultracold dilute Bose gas, m different hyperfine spin states may repel each other and form separate nodal domains, such a phenomenon, called phase separation of a multiple mixture of BEC, has been extensively investigated by experimental and theoretical physicists (13; 26; 29). From (3; 19), a large repulsive inter-component scattering length may cause spontaneous symmetry bifurcation which makes phase separation happen. Here a positive and large inter-component scattering length can be obtained by adjusting the externally applied magnetic field because of Feshblack resonance (25).

For the study of numerical computation, based on schemes of (5; 6; 7), a normalized gradient flow (NGF), monotone scheme and a time-splitting sine-spectral (TSSP) method have been developed by (4) for computing ground states of a multi-component BEC by solving time-dependent CGPEs (1.1). The NGF method was proven to preserve energy diminishing property in the linear case (4; 5). The TSSP method is explicit, unconditionally stable, time reversible and time transverse invariant (4). Recently, a Gauss-Seidel-type iteration (GSI) has been proposed by (14) for computing ground states of a multi-component BEC by solving the time-independent CGPEs (1.4). It was proven that the GSI method convergent locally and linearly to a fixed point if and only if the associated minimized energy functional problem has a strictly local minimum at the feasible fixed point.

The main purpose of this paper is first to discretize the time-independent CGPEs (1.4) to a nonlinear algebraic eigenvalue problem (NAEP) and to develop a structured continuation method based on the classical continuation method (2; 27) for the computation of possibly all positive bound states of a multi-component BEC. Second, in order to utilize the sparsity and the block structure of the associated NAEP, we propose a continuation method combined with the BSOR iteration (33, p. 594-596) and the Lanczos-Galerkin projection method (30; 31) for tracing the solution curve of the NAEP. Third,

we prove that the primal stalk of the solution curve of the NAEP coincides with the unique global minimizer of a single-component BEC which is represented by an initial value ODE. Furthermore, we prove that the solution curve of the NAEP will encounter a first bifurcation point at a finite value of the repulsive scattering length. For the case of $m = 2$, we also prove that two identical ground states will bifurcate into two different ground states which are symmetric with respect to some suitable axis in Ω.

To compare with the GSI method in (14) we note that the continuation BSOR-Lanczos-Galerkin method is used to compute possibly all positive bound state solutions of a multi-component BEC, i.e., possibly all eigensolutions of NAEP, in spite of that the positive bound state solution is stable for the negative gradient flow of $E(\boldsymbol{\phi})$ in (1.5), i.e., in spite of that the positive bound state solution is the ground state solution (the minimal solution) of (1.5). On the other hand, the GSI method (14) is used to find the ground state solution of a multi-component BEC.

This paper is organized as follows. In Section 2, we first develop a continuation BSOR-Lanczos-Galerkin method for solving the NAEP. Then, we propose an efficient detection for testing the singularity of the solution curve. In Section 3, we prove the existence of the bifurcation of a multi-component BEC, whenever the repulsive scattering length becomes sufficiently large. Numerical results of positive bound state solutions of a two/three-component BEC by solving the NAEP are presented in Section 4. Finally, a conclusion is given in Section 5.

Throughout this paper, we use the bold face letters or symbols to denote a matrix or a vector. For $\mathbf{u} = (u_1, \ldots, u_N)^\top$, $\mathbf{v} = (v_1, \ldots, v_N)^\top \in \mathbb{R}^N$, $\mathbf{u} \circ \mathbf{v} = (u_1 v_1, \ldots, u_N v_N)^\top$ denotes the Hadamard product of $\mathbf{u}$ and $\mathbf{v}$, $\mathbf{u}^{\circledcirc r} = \mathbf{u} \circ \cdots \circ \mathbf{u}$ denotes the r-time Hadamard product of $\mathbf{u}$, $[\![\mathbf{u}]\!] := \mathrm{diag}(\mathbf{u})$ denotes the diagonal matrix of $\mathbf{u}$. For $\mathbf{A} \in \mathbb{R}^{M \times N}$, $\mathbf{A} > 0$ (≥ 0) denotes a positive (nonnegative) matrix with positive (nonnegative) entries, $\mathbf{A} \succ 0$ (with $\mathbf{A}^\top = \mathbf{A}$) denotes a symmetric positive definite matrix and $\sigma(\mathbf{A})$ denotes the spectrum of $\mathbf{A}$.

2 Continuation BSOR-Lanczos-Galerkin algorithm

For convenience, hereafter we assume that Ω in (1.4a) is contained in $\mathbb{R}^2$. To solve the nonlinear eigenvalue problem (1.4) numerically by continuation methods (e.g. (2; 27)), it is natural to first discretize the differential equations in (1.4) by a finite difference method or a finite element method. Suppose that the Laplacian operator $-\nabla^2$ in (1.4a) is discretized by the central difference approximation with the grid size h. Then, due to the Dirichlet boundary condition (1.1c) the discretization matrix, denoted by $\mathbf{A} \in \mathbb{R}^{N \times N}$ corresponding to the operator $-\nabla^2$, is an irreducible and symmetric positive definite matrix

with nonpositive off-diagonal entries (i.e. an irreducible symmetric M-matrix). By $\frac{1}{h}\mathbf{u}_j$ and $\mathbf{V}_j \in \mathbb{R}^N$, respectively, are denoted the approximations of the j-th wave function $\phi_j(\mathbf{x})$ and the j-th trapping potential $V_j(\mathbf{x})$, for $j = 1, \ldots, m$. Rewrite α_j and β_{kj} in (1.4) by $\alpha_j := \alpha_j/h^2$ and $\beta_{kj} := \beta_{kj}/h^2$, respectively, then the discretization of (1.4), referred to a nonlinear algebraic eigenvalue problem (NAEP), can be formulated as follows

$$\mathbf{A}\mathbf{u}_j + \mathbf{V}_j \circ \mathbf{u}_j + \alpha_j \mathbf{u}_j^{②} \circ \mathbf{u}_j + \sum_{k\neq j, k=1}^{m} \beta_{kj} \mathbf{u}_k^{②} \circ \mathbf{u}_j = \lambda_j \mathbf{u}_j, \tag{2.1a}$$

$$\mathbf{u}_j^\top \mathbf{u}_j = 1, \ j = 1, \ldots, m. \tag{2.1b}$$

The energy functional $E(\boldsymbol{\phi})$ in (1.5b) becomes

$$E(\mathbf{u}) = \sum_{j=1}^{m} \left(\frac{1}{2} \mathbf{u}_j^\top \mathbf{A} \mathbf{u}_j + \frac{1}{2} \mathbf{V}_j^\top \mathbf{u}_j^{②} + \frac{\alpha_j}{4} \mathbf{u}_j^{②\top} \mathbf{u}_j^{②} \right) + \frac{1}{4} \sum_{k,j=1, k\neq j}^{m} \beta_{kj} \mathbf{u}_k^{②\top} \mathbf{u}_j^{②}, \tag{2.2}$$

where $\mathbf{u} = (\mathbf{u}_1, \ldots, \mathbf{u}_m)$. The eigenvalue vector $\boldsymbol{\lambda} = (\lambda_1, \ldots, \lambda_m)$ and the associated eigenvectors $\{\mathbf{u}_1, \ldots, \mathbf{u}_m\}$ satisfy

$$\sum_{j=1}^{m} \lambda_j = 2E(\mathbf{u}) + \frac{1}{2} \sum_{k,j=1, k\neq j}^{m} \beta_{kj} \mathbf{u}_k^{②\top} \mathbf{u}_j^{②} + \frac{1}{2} \sum_{j=1}^{m} \alpha_j \mathbf{u}_j^{②\top} \mathbf{u}_j^{②}. \tag{2.3}$$

To study the phase separation of a multi-component BEC, we assume that the intra- and inter-component scattering lengths α_j's and β_{kj}'s in (2.1a) satisfy

$$\alpha_j = \alpha := \alpha_0 + \mu_0 p, \ j = 1, \ldots, m, \tag{2.4a}$$

$$\beta_{kj} = \beta_{jk} = \beta := \beta_0 + \nu_0 p, \ k \neq j, \ k, j = 1, \ldots, m, \tag{2.4b}$$

where α_0, μ_0, β_0 and ν_0 are given nonnegative constants, and p is a positive parameter. Let

$$\mathbf{x} = (\mathbf{u}_1^\top, \lambda_1, \ldots, \mathbf{u}_m^\top, \lambda_m)^\top. \tag{2.5}$$

Then the NAEP of (2.1) can be rewritten by the parameter-dependent form

$$\mathbf{G}(\mathbf{x}, p) = 0, \tag{2.6}$$

where $\mathbf{G} \equiv (\mathbf{G}_1, g_1, \ldots, \mathbf{G}_m, g_m) : \mathbb{R}^{(N+1)m} \times \mathbb{R} \to \mathbb{R}^{(N+1)m}$ is a smooth mapping with

$$\mathbf{G}_j(\mathbf{x}, p) = \mathbf{A}\mathbf{u}_j + \mathbf{V}_j \circ \mathbf{u}_j + \alpha \mathbf{u}_j^{②} \circ \mathbf{u}_j + \beta \sum_{k\neq j}^{m} \mathbf{u}_k^{②} \circ \mathbf{u}_j - \lambda_j \mathbf{u}_j, \tag{2.7a}$$

$$g_j(\mathbf{x}, p) = \frac{1}{2}(\mathbf{u}_j^\top \mathbf{u}_j - 1), \tag{2.7b}$$

for $j = 1, \ldots, m$. We denote the Jacobian of $\mathbf{G}$ by

$$\mathcal{D}\mathbf{G} = [\mathbf{G}_{\mathbf{x}}, \mathbf{G}_p] = [\mathbf{G}_{\mathbf{x}}, \mathbf{G}_\alpha \mu_0 + \mathbf{G}_\beta \nu_0] \in \mathbb{R}^{M \times (M+1)}$$

with $M = (N+1)m$, and the solution curve $\boldsymbol{\mathcal{C}}$ of (2.6) by

$$\boldsymbol{\mathcal{C}} = \{\mathbf{y}(s) = (\mathbf{x}(s)^\top, p(s))^\top |\ \mathbf{G}(\mathbf{y}(s)) = 0,\ s \in \mathbf{J} \subseteq \mathbb{R}\}. \tag{2.8}$$

Here we assume a parametrization via arc lengths is available on $\boldsymbol{\mathcal{C}}$. By differentiating the equation (2.6) with respect to s we obtain

$$\mathcal{D}\mathbf{G}(\mathbf{y}(s))\dot{\mathbf{y}}(s) = 0,$$

where $\dot{\mathbf{y}}(s) = (\dot{\mathbf{x}}(s)^\top, \dot{p}(s))^\top$ denotes a tangent vector to $\boldsymbol{\mathcal{C}}$ at $\mathbf{y}(s)$.

Several well-known curve-tracking algorithms have been developed during the past decades, e.g., the HOMPACK of Watson et al. (34) and the book of numerical methods for bifurcations by Govaerts (23). Recently, Davidson (17) employed a preconditioned version of the recursive projection method in the context of continuation method for computing bifurcation scenario of large scale parameter-dependent problems. In the following, we will trace the solution curve $\boldsymbol{\mathcal{C}}$ in (2.8) by predictor-corrector continuation methods (2; 27) combined with BSOR iteration (33, p. 594-596) and Lanczos-Galerkin projection method (30; 31), which is referred to a continuation BSOR-Lanczos-Galerkin method.

Let $\mathbf{y}_i = (\mathbf{x}_i^\top, p_i)^\top \in \mathbb{R}^{M+1}$ be a point that has been accepted as an approximating point for the solution curve $\boldsymbol{\mathcal{C}}$. Suppose that the Euler predictor, i.e.,

$$\mathbf{y}_{i+1,1} = \mathbf{y}_i + h_i \dot{\mathbf{y}}_i$$

is used to predict a new point $\mathbf{y}_{i+1,1}$, where $h_i > 0$ is the step length and $\dot{\mathbf{y}}_i$ is the unit tangent vector at $\mathbf{y}_i$ which is obtained by solving the linear bordered system

$$\left[\begin{array}{c|c} \mathbf{G}_{\mathbf{x}}(\mathbf{y}_i) & \mathbf{G}_p(\mathbf{y}_i) \\ \hline \multicolumn{2}{c}{\mathbf{c}_i^\top} \end{array}\right] \dot{\mathbf{y}}_i = \begin{bmatrix} \bar{\mathbf{0}} \\ 1 \end{bmatrix} \tag{2.9}$$

with some suitable constant vector $\mathbf{c}_i \in \mathbb{R}^{M+1}$. The accuracy of the approximation $\mathbf{y}_{i+1,1}$ to the solution curve $\boldsymbol{\mathcal{C}}$ can be improved by a correction process. Typically, Newton's method is chosen as a corrector, i.e., the following linear bordered system

$$\left[\begin{array}{c|c} \mathbf{G}_{\mathbf{x}}(\mathbf{y}_{i+1,l}) & \mathbf{G}_p(\mathbf{y}_{i+1,l}) \\ \hline \multicolumn{2}{c}{\dot{\mathbf{y}}_i^\top} \end{array}\right] \boldsymbol{\delta}_l = \begin{bmatrix} -\mathbf{G}(\mathbf{y}_{i+1,l}) \\ \rho_l \end{bmatrix},\ l = 1, 2, \ldots, \tag{2.10}$$

with $\rho_l = \dot{\mathbf{y}}_i^\top(\mathbf{y}_{i+1,l} - \mathbf{y}_{i+1,1})$, is solved by setting $\mathbf{y}_{i+1,l+1} = \mathbf{y}_{i+1,l} + \boldsymbol{\delta}_l$, $l = 1, 2, \ldots$. If $\{\mathbf{y}_{i+1,l}\}$ converges until $l = l_\infty$, then we accept $\mathbf{y}_{i+1} = \mathbf{y}_{i+1,l_\infty}$ as a new approximation to the solution curve $\boldsymbol{\mathcal{C}}$.

In fact, linear systems (2.9) and (2.10) can be rewritten in the form

$$\begin{bmatrix} \mathbf{B} & \mathbf{f} \\ \mathbf{g}^\top & \gamma \end{bmatrix} \begin{bmatrix} \mathbf{x} \\ \sigma \end{bmatrix} = \begin{bmatrix} \mathbf{q} \\ \rho \end{bmatrix}, \tag{2.11}$$

where $\mathbf{B} \in \mathbb{R}^{M\times M}$, $\mathbf{f}, \mathbf{g}$ and $\mathbf{q} \in \mathbb{R}^M$. The linear system (2.11) can be easily solved by the well-known block elimination (BE) algorithm (see e.g., (27)) when $\mathbf{B}$ is well-conditioned. However, near turning points or branch points. $\mathbf{B}$ in (2.11) becomes nearly singular, i.e., $\mathbf{B}$ is ill-conditioned. Then the linear system should be solved by the deflated block elimination (DBE) algorithm by Chan (12), or the more efficient, backward stable, mixed block elimination (BEM) algorithm proposed by Govaerts (21; 22).

Algorithm 2.1 Mixed Block Elimination (BEM).

(i) Solve $\boldsymbol{\xi}^\top \mathbf{B} = \mathbf{g}^\top$,
(ii) Compute $\delta_1 = \gamma - \boldsymbol{\xi}^\top \mathbf{f}$, $\sigma = (\rho - \boldsymbol{\xi}^\top \mathbf{q})/\delta_1$,
(iii) Solve $\mathbf{B}\mathbf{v} = \mathbf{f}$,
(iv) Compute $\delta = \gamma - \mathbf{g}^\top \mathbf{v}$, $\mathbf{q}_1 = \mathbf{q} - \mathbf{f}\sigma$, $\rho_1 = \rho - \gamma\sigma$,
(v) Solve $\mathbf{B}\mathbf{w} = \mathbf{q}_1$,
(vi) Compute $\sigma_1 = (\rho_1 - \boldsymbol{\xi}^\top \mathbf{w})/\delta$,
(vii) Compute $\mathbf{x} = \mathbf{w} - \mathbf{v}\sigma_1$, $\sigma = \sigma + \sigma_1$.

From Algorithm 2.1, we see that the main step in (2.9) or in (2.10) is to solve a linear system of the form $\mathbf{G}_{\mathbf{x}}(\mathbf{y})\boldsymbol{\xi} = \mathbf{g}$, where $\mathbf{y} = (\mathbf{x}^\top, p)^\top$ and $\mathbf{x}$ is given in (2.5). By (2.6) and (2.7) these linear systems can be formulated into the form

$$\mathbf{B}\boldsymbol{\xi} \equiv \begin{bmatrix} \mathbf{B}_{11} & \mathbf{B}_{12} & \cdots & \mathbf{B}_{1m} \\ \mathbf{B}_{21} & \mathbf{B}_{22} & \cdots & \mathbf{B}_{2m} \\ \vdots & \vdots & \ddots & \vdots \\ \mathbf{B}_{m1} & \mathbf{B}_{m2} & \cdots & \mathbf{B}_{mm} \end{bmatrix} \begin{bmatrix} \boldsymbol{\xi}_1 \\ \boldsymbol{\xi}_2 \\ \vdots \\ \boldsymbol{\xi}_m \end{bmatrix} = \begin{bmatrix} \mathbf{g}_1 \\ \mathbf{g}_2 \\ \vdots \\ \mathbf{g}_m \end{bmatrix}, \tag{2.12}$$

where

$$\begin{aligned} \mathbf{B}_{jj} &= \mathcal{D}_{(\mathbf{u}_j,\lambda_j)} \begin{bmatrix} \mathbf{G}_j(\mathbf{y}) \\ \mathbf{g}_j(\mathbf{y}) \end{bmatrix} \\ &= \left[\begin{array}{c|c} \mathbf{A} + [\![\mathbf{V}_j + 3\alpha\mathbf{u}_j^{②} + \beta\sum_{k\neq j}\mathbf{u}_k^{②}]\!] - \lambda_j I & \mathbf{u}_j \\ \hline \mathbf{u}_j^\top & 0 \end{array}\right] \equiv \left[\begin{array}{c|c} \mathbf{A}_j & \mathbf{u}_j \\ \hline \mathbf{u}_j^\top & 0 \end{array}\right] \end{aligned} \tag{2.13a}$$

and

$$\mathbf{B}_{kj} = \mathcal{D}_{(\mathbf{u}_k,\lambda_k)} \begin{bmatrix} \mathbf{G}_j(\mathbf{y}) \\ \mathbf{g}_j(\mathbf{y}) \end{bmatrix} = \left[\begin{array}{c|c} 2\beta[\![\mathbf{u}_k \circ \mathbf{u}_j]\!] & 0 \\ \hline 0 & 0 \end{array}\right], \ k \neq j, \ k, j = 1, \ldots, m. \tag{2.13b}$$

Note that the matrix $\mathbf{B}$ in (2.12) is symmetric.

Since only positive bound states of a multi-component BEC are of interest, the eigenvectors $\{\mathbf{u}_j\}_{j=1}^m$ in (2.1) are restricted to be positive. By applying Perron-Fronbenius Theorem (see e.g., (10, p.27)) to the irreducible symmetric M-matrix $\widehat{\mathbf{A}}_j \equiv (\mathbf{A} + [\![\mathbf{V}_j + \alpha \mathbf{u}_j^{②} + \beta \sum_{k \neq j} \mathbf{u}_k^{②}]\!])$, we have that the eigenvalue λ_j in (2.1a) is the unique minimal eigenvalue of $\widehat{\mathbf{A}}_j$ associated with the positive eigenvector $\mathbf{u}_j$. This implies that the matrix $\mathbf{A}_j = \widehat{\mathbf{A}}_j + 2[\![\alpha_j \mathbf{u}_j^{②}]\!]$ defined in (2.13a) is symmetric positive definite, and thus, $\mathbf{B}_{jj}$ in (2.13a) is invertible and is a bordered matrix as in (2.11), for $j = 1, \ldots, m$. With this property, the linear system (2.12) can be simply solved by the block SOR algorithm (33, p. 594-596).

Algorithm 2.2 Block SOR (BSOR).

(i) Choose a suitable parameter $\omega \in (1, 2)$ and starting vectors $\{\boldsymbol{\xi}_j^{(0)}\}_{j=1}^m$, $i = 0$;

(ii) Repeat i : until convergence,
For $j = 1, \ldots, m$,
solve the linear system

$$\mathbf{B}_{jj}\boldsymbol{\xi}_j^{(i+1)} = \omega \left[\mathbf{f}_j - \sum_{k>j} \mathbf{B}_{jk}\boldsymbol{\xi}_k^{(i)} - \sum_{k<j} \mathbf{B}_{jk}\boldsymbol{\xi}_k^{(i+1)} \right] + (1-\omega)\mathbf{B}_{jj}\boldsymbol{\xi}_j^{(i)} \tag{2.14}$$

for $\boldsymbol{\xi}_j^{(i+1)}$ by using BEM algorithm (algorithm 2.1),
end for j;

(iii) If converges, then $\boldsymbol{\xi}_j \leftarrow \boldsymbol{\xi}_j^{(i+1)}$ $(j = 1, \ldots, m)$, stop;
else $i \leftarrow i + 1$, Goto Repeat (ii).

We now reduce our problem of (2.11) to solving several symmetric linear systems of the form

$$\mathbf{A}_j\boldsymbol{\xi}^{(i)} = \mathbf{b}^{(i)}, \ i = 1, \ldots, r, \tag{2.15}$$

involving the same $N \times N$ matrix $\mathbf{A}_j$ but different right-hand sides $\mathbf{b}^{(i)}$. Furthermore, the right-hand sides are not available at the same time, i.e., a given right-hand side $\mathbf{b}^{(i)}$ depends on the solution $\boldsymbol{\xi}^{(l)}$, $l = 1, \ldots, i-1$, of the previous

linear systems. For this situation, Parlett (30) suggested using the Lanczos algorithm to solve the first system and saving the generated Lanczos vectors for providing good approximate solutions to the subsequent systems. An approximate solution to the second linear system can then be obtained by using a Galerkin projection technique onto the Krylov subspace generated when solving the first linear system. If the approximate solution obtained in this way is not accurate enough, it can be improved by the restarted Lanczos-Galerkin procedure (31) which has been shown to be equivalent to the block Lanczos algorithm (24). By repeating the process described above, we can solve the subsequent linear systems in (2.15) after the first linear system is solved.

Algorithm 2.3 Lanczos-Galerkin Projection Method.

(i) First pass.
Solve the first linear system $\mathbf{A}_j\boldsymbol{\xi}^{(1)} = \mathbf{b}^{(1)}$ by q-step Lanczos algorithm (see e.g., (30));
Let $\mathbf{V}_q = [\mathbf{v}_1, \ldots, \mathbf{v}_q]$ be the orthogonal Lanczos basis spanning the Krylov subspace with $\mathbf{v}_1 = (\mathbf{b}^{(1)} - \mathbf{A}_j\boldsymbol{\xi}_0^{(1)})/\|\mathbf{b}^{(1)} - \mathbf{A}_j\boldsymbol{\xi}_0^{(1)}\|$ and $\mathbf{T}_q$ be the corresponding $q \times q$ tridiagonal matrix;

(ii) Second pass.
For $i = 2, \ldots, r$,
Compute $\mathbf{r}_0^{(i)} = \mathbf{b}^{(i)} - \mathbf{A}_j\boldsymbol{\xi}_0^{(i)}$ with an appropriate initial $\boldsymbol{\xi}_0^{(i)}$,
Compute $\boldsymbol{\xi}^{(i)} = \boldsymbol{\xi}_0^{(i)} + \mathbf{V}_q\mathbf{T}_q^{-1}\mathbf{V}_q^\top\mathbf{v}_0^{(i)}$,
If the accuracy of the approximation $\boldsymbol{\xi}^{(i)}$ is not sufficient, perform a refinement (restarted or block) Lanczos-Galerkin process (see (31) for details),
end for i.

Testing for Bifurcation.

Let $\boldsymbol{\mathcal{C}}$ be the path defined in (2.8). As was described in (2; 23; 27) a point $\mathbf{y}(s) \in \boldsymbol{\mathcal{C}}$ is said to be a regular point if $\operatorname{rank}(\mathcal{D}\mathbf{G}(\mathbf{y}(s))) = M$, and is a singular point if $\operatorname{rank}(\mathcal{D}\mathbf{G}(\mathbf{y}(s))) \leq M-1$. For a regular point $\mathbf{y}(s)$, the tangent vector $\dot{\mathbf{y}}(s)$ is uniquely determined by the linear system (2.9). We now consider that the path $\boldsymbol{\mathcal{C}}$ undergoes a singular point $(\mathbf{x}(s_0), p(s_0))$ and give methods to jump over such a point. In Theorem 3.2 (See Section 3 later!) we shall prove that $\dim\mathcal{N}(\mathbf{G}_\mathbf{x}(s_0)) \geq m-1$.

(I) Case $m = 2$.
One can see that in (27, p. 97) a point $(\mathbf{x}(s_0), p(s_0)) \in \boldsymbol{\mathcal{C}}$ is a simple singular point if and only if either

$$\text{(a)}\quad \dim\mathcal{N}(\mathbf{G}_\mathbf{x}(s_0)) = 1,\ \mathbf{G}_p(s_0) \in \mathcal{R}(\mathbf{G}_\mathbf{x}(s_0)) \ \text{ or} \tag{2.16}$$

$$\text{(b)}\quad \dim\mathcal{N}(\mathbf{G}_\mathbf{x}(s_0)) = 2,\ \mathbf{G}_p(s_0) \notin \mathcal{R}(\mathbf{G}_\mathbf{x}(s_0)). \tag{2.17}$$

Here $\mathcal{N}$ and $\mathcal{R}$ denote the null and range spaces of $\mathbf{G}_{\mathbf{x}}(s_0)$, respectively.

However, the case (b) of (2.17) rarely happens because in generic systems it has codimension 4, i.e., it can only be expected in systems with four free parameters. However, it cannot be expected in a situation of the NAEP (2.1) with equivariant parameters. (see (23) for details).

(II) Case $m \geq 3$.
As in (I), for simplicity, here we only consider the case

$$\dim \mathcal{N}(\mathbf{G}_{\mathbf{x}}(s_0)) = m-1,\ \mathbf{G}_p(s_0) \in \mathcal{R}(\mathbf{G}_{\mathbf{x}}(s_0)).$$

Algorithm 2.4 Tangent Vectors at Singularity.

(I) For $m = 2$ (27, p. 88-99):
  (i) Compute the unit right and left null vectors $\boldsymbol{\phi}$ and $\boldsymbol{\psi}$ of $\mathbf{G}_{\mathbf{x}}(s_0)$, respectively, and solve $\mathbf{G}_{\mathbf{x}}(s_0)\boldsymbol{\phi}_0 = -\mathbf{G}_p(s_0)$ with $\boldsymbol{\phi}^\top \boldsymbol{\phi}_0 = 0$, by using sparse SVDPACK (11);
  (ii) Form $\boldsymbol{\phi}_1 = \begin{pmatrix} \boldsymbol{\phi} \\ 0 \end{pmatrix}$ and $\boldsymbol{\phi}_2 = \begin{pmatrix} \boldsymbol{\phi}_0 \\ 1 \end{pmatrix}$;
  (iii) Solve the real vector roots $\{(\hat{\mu}_k, \hat{\nu}_k)\}_{k=1}^2$ of $a_{11}\mu^2 + 2a_{12}\mu\nu + a_{22}\nu^2$ with

$$a_{11} = \boldsymbol{\psi}^\top \mathbf{G}_{\mathbf{xx}}(s_0)\boldsymbol{\phi}\boldsymbol{\phi},\ a_{12} = \boldsymbol{\psi}^\top[\mathbf{G}_{\mathbf{xx}}(s_0)\boldsymbol{\phi}_0 + \mathbf{G}_{\mathbf{x}p}]\boldsymbol{\phi},$$
$$a_{22} = \boldsymbol{\psi}^\top[\mathbf{G}_{\mathbf{xx}}(s_0)\boldsymbol{\phi}_0\boldsymbol{\phi}_0 + 2\mathbf{G}_{\mathbf{x}p}(s_0)\boldsymbol{\phi}_0 + \mathbf{G}_{pp}(s_0)];$$

  (iv) Form tangent vectors $\dot{\mathbf{y}}_k(s_0) = \hat{\mu}_k\boldsymbol{\phi}_1 + \hat{\nu}_k\boldsymbol{\phi}_2$, $k = 1, 2$.

(II) For $m \geq 3$:
  (i) Compute the unit right null vectors $\boldsymbol{\phi}^{(1)}, \ldots, \boldsymbol{\phi}^{(m-1)}$ of $\mathbf{G}_{\mathbf{x}}(s_0)$, and solve $\mathbf{G}_{\mathbf{x}}(s_0)\boldsymbol{\phi}_0 = -\mathbf{G}_p(s_0)$ with ${\boldsymbol{\phi}^{(k)}}^\top \boldsymbol{\phi}_0 = 0$, $k = 1, \ldots, m-1$, by using sparse SVDPACK (11);
  (ii) Form $\boldsymbol{\phi}_k = \begin{pmatrix} \boldsymbol{\phi}^{(k)} \\ 0 \end{pmatrix}$, $k = 1, \ldots, m-1$ and $\boldsymbol{\phi}_m = \begin{pmatrix} \boldsymbol{\phi}_0 \\ 1 \end{pmatrix}$;
  (iii) Form trial tangent vectors $\dot{\mathbf{y}}_k(s_0) = \boldsymbol{\phi}_k$, $k = 1, \ldots, m-1$ and $\dot{\mathbf{y}}_m(s_0) = \boldsymbol{\phi}_m$.

Now our task is to design algorithms to detect singular points of the solution curve $\boldsymbol{\mathcal{C}}$ and to compute $\boldsymbol{\phi}_k$'s in Algorithm 2.4 for tangent vectors. In practice, in step (iii) of the case of $m \geq 3$ we usually choose any one trial tangent vector $\dot{\mathbf{y}}_k(s_0)$, $k \in \{1, \ldots, m-1\}$, for following the branch of the solution curve.

In fact, by the path following process (2.9), Algorithm 2.2 combined with Algorithm 2.3 can also be used to compute the smallest eigenvalue in modulo of $\mathbf{G}_{\mathbf{x}}(s_i)$, say $\mu(s_i)$, and further to detect the singularity of $\boldsymbol{\mathcal{C}}$. It leads to the

following algorithm, which is referred to as an inverse power method.

Algorithm 2.5 Inverse Power Method.

(i) Given a unit vector $\boldsymbol{\zeta}_0 = (\boldsymbol{\zeta}_1^{(0)\top}, \ldots, \boldsymbol{\zeta}_m^{(0)\top})^\top \in \mathbb{R}^{(M+1)m}$, and let $l = 1$,
(ii) Repeat l: until convergence,
Call Algorithm 2.2 and Algorithm 2.3 to solve $\mathbf{B}\widehat{\boldsymbol{\zeta}}_l = \boldsymbol{\zeta}_{l-1}$, where $\mathbf{B}$ is given in (2.12). Set

$$\boldsymbol{\zeta}_l = \widehat{\boldsymbol{\zeta}}_l / \|\widehat{\boldsymbol{\zeta}}_l\|_2, \quad \mu^{(l)} = \boldsymbol{\zeta}_l^\top \mathbf{B} \boldsymbol{\zeta}_l;$$

(iii) If converges, then $\mu(s) \leftarrow \mu^{(l)}$; else $l \leftarrow l + 1$, Goto Repeat (ii).

Let $\mu(s_1)$ and $\mu(s_2)$ be the smallest eigenvalues in modulus of $\mathbf{G}_{\mathbf{x}}(\mathbf{y}(s_1))$ and $\mathbf{G}_{\mathbf{x}}(\mathbf{y}(s_2))$, respectively, where $s_1 < s_2$ are two consecutive parameters. If $\mu(s_1) > 0$ and $\mu(s_2) < 0$, then there is a $s^* \in (s_1, s_2)$ such that $\mathbf{G}_{\mathbf{x}}(\mathbf{y}(s^*))$ is singular. We propose the following algorithm to detect the singular point of $\boldsymbol{\mathcal{C}}$.

Algorithm 2.6 Detection of Singularity of $\boldsymbol{\mathcal{C}}$.

(i) Given $\mu(s_i)$ the smallest eigenvalue in modulus of $\mathbf{G}_{\mathbf{x}}(\mathbf{y}(s_i))$, $i = 1, 2$, where $\mu(s_1) > 0$, $\mu(s_2) < 0$, e.g., $|\mu(s_1)| \approx |\mu(s_2)| \approx 10^{-4}$.
(ii) Do Secant Method: until convergence,
(a) Compute $\mathbf{y}_1(s^*) := \mathbf{y}(s^*) = \mathbf{y}(s_1) + \dfrac{\mathbf{t}^* \mu(s_1)}{\mu(s_2) - \mu(s_1)}$,
where $\mathbf{t}^* = \mathbf{y}(s_1) - \mathbf{y}(s_2)$,
(b) Perform Newton Correction (2.10): until convergence (i.e., $\ell = \ell_\infty$),
Solve

$$\left[\begin{array}{c|c} \mathbf{G}_{\mathbf{x}}(\mathbf{y}_\ell(s^*)) & \mathbf{G}_p(\mathbf{y}_\ell(s^*)) \\ \hline \multicolumn{2}{c}{\mathbf{t}^*} \end{array}\right] \boldsymbol{\delta}_\ell = \left[\begin{array}{c} -\mathbf{G}(\mathbf{y}_\ell(s^*)) \\ \hline \rho_\ell \end{array}\right]$$

with $\rho_\ell = \mathbf{t}^{*\top}(\mathbf{y}_\ell(s^*) - \mathbf{y}_1(s^*))$,
set $\mathbf{y}_{\ell+1}(s^*) = \mathbf{y}_\ell(s^*) + \boldsymbol{\delta}_\ell$, $\ell \leftarrow \ell + 1$, Goto (b).
(c) Compute $\mu(s^*)$ of $\mathbf{G}_{\mathbf{x}}(\mathbf{y}_{\ell_\infty}(s^*))$ using Algorithm 2.5,
(d) If $|\mu(s^*)| <$Tol, then perform (iii), else
(e) If $\mu(s^*) > 0$, $s_1 \leftarrow s^*$, else $s_2 \leftarrow s^*$, Goto (ii);
(iii) Call Algorithm 2.4 to compute the desired tangent vectors with $\mathbf{y}(s_0) = \mathbf{y}_{\ell_\infty}(s^*)$.

By combining Algorithm 2.1−2.6, it leads to our continuation BSOR-Lanczos-Galerkin algorithm which can be used to compute possibly all positive bound states of a multi-component BEC.

3 Bifurcation of a Multi-Component BEC

For a multi-component BEC, it is well-known (3; 19) that a large repulsive inter-component scattering length may set in spontaneous symmetry breaking inducing phase separation. It was shown in (14) that m components of positive bound states may repel each other and form segregated nodal domains as the repulsive scattering lengths go to infinity. In fact, the NAEP of (2.1) always has identical bound state solutions, i.e., $\mathbf{u}_1 = \cdots = \mathbf{u}_m$, provided that $\mathbf{V}_j = \mathbf{V}$, $\alpha_j = \alpha$, $\beta_{kj} = \beta$ $(k \neq j)$, for $k, j = 1, \ldots, m$. For this situation, we shall prove that the solution curve $\boldsymbol{\mathcal{C}}$ of (2.8) with $\alpha = \alpha_0$ fixed will undergo a bifurcation point at a finite value $\beta = \beta^* > 0$. For $m = 2$, we further prove that two identical ground states will bifurcate into two different ground states which are symmetric with respect to some suitable axis in Ω. To this end, we first study the ground states of a single-component BEC (i.e. $m = 1$) described by the NAEP

$$\mathbf{A}\mathbf{u} + \mathbf{V} \circ \mathbf{u} + \alpha \mathbf{u}^{②} \circ \mathbf{u} = \lambda \mathbf{u}, \tag{3.1a}$$

$$\mathbf{u}^\top \mathbf{u} = 1. \tag{3.1b}$$

The ground state solutions can naturally be solved by the continuation method. From (2.2) we see that the associated energy functional of (3.1) becomes

$$E_\alpha(\mathbf{u}) = \frac{1}{2}\mathbf{u}^\top \mathbf{A}\mathbf{u} + \frac{1}{2}\mathbf{V}^\top \mathbf{u}^{②} + \frac{\alpha}{4}\mathbf{u}^{②\top}\mathbf{u}^{②}. \tag{3.2}$$

The next theorem proves that the unique global minimizer of $E_\alpha(\mathbf{u})$ exists and satisfies an initial value problem (IVP).

Theorem 3.1 *The optimization problem*

$$\min\{E_\alpha(\mathbf{u})|\ \mathbf{u}^\top \mathbf{u} = 1,\ \mathbf{u} > 0 \in \mathbb{R}^N\} \tag{3.3}$$

has a unique global minimizer $\mathbf{u}(\alpha)$ *which satisfies the initial value problem (IVP):*

$$\dot{\mathbf{u}}(\alpha) = -\bar{\mathbf{A}}^{-1}(\alpha)\mathbf{u}^{③}(\alpha) + \bar{\mathbf{A}}^{-1}(\alpha)\frac{\mathbf{u}^\top(\alpha)\bar{\mathbf{A}}^{-1}(\alpha)\mathbf{u}^{③}(\alpha)}{\mathbf{u}^\top(\alpha)\bar{\mathbf{A}}^{-1}(\alpha)\mathbf{u}(\alpha)}\mathbf{u}(\alpha) \tag{3.4}$$

with $\mathbf{u}(0)$ *being the eigenvector of* $\mathbf{A} + [\![\mathbf{V}]\!]$ *to the minimal eigenvalue, where* $\bar{\mathbf{A}}(\alpha) \equiv \mathbf{A} + [\![\mathbf{V} + 3\alpha\mathbf{u}^{②}(\alpha)]\!] - \lambda(\alpha)\mathbf{I}_N$ *and* $\lambda(\alpha)$ *is the minimal eigenvalue of* $\mathbf{A} + [\![\mathbf{V} + \alpha\mathbf{u}^{②}(\alpha)]\!]$. *Furthermore,* $\mathbf{u}(\alpha) \to \frac{1}{\sqrt{N}}\mathbf{e}$, *as* $\alpha \to \infty$, *where* $\mathbf{e} = (1, \ldots, 1)^\top$.

PROOF. We first prove that $\mathbf{u}(\alpha)$ satisfies (3.4) by continuation method. Differentiating the equation in (3.1) with respect to α formally, we obtain

$$\begin{bmatrix} \bar{\mathbf{A}}(\alpha) & \mathbf{u} \\ \mathbf{u}^\top & 0 \end{bmatrix} \begin{bmatrix} \dot{\mathbf{u}} \\ -\dot{\lambda} \end{bmatrix} \equiv \left[\begin{array}{c|c} \mathbf{A} + [\![\mathbf{V} + 3\alpha \mathbf{u}^{②}]\!] - \lambda \mathbf{I} & \mathbf{u} \\ \hline \mathbf{u}^\top & 0 \end{array}\right] \begin{bmatrix} \dot{\mathbf{u}} \\ -\dot{\lambda} \end{bmatrix} = \begin{bmatrix} -\mathbf{u}^{③} \\ 0 \end{bmatrix}. \quad (3.5)$$

It is easily seen that the matrix $\mathbf{A} + [\![\mathbf{V}]\!]$ has a positive eigenvector $\mathbf{u}(0) > 0$ corresponding to the positive minimal eigenvalue $\lambda(0)$, whenever $\alpha = 0$. By Implicit Function Theorem and the positivity of $\mathbf{u}(0)$, there exists an $\alpha_1 > 0$ such that $(\mathbf{u}(\alpha), \lambda(\alpha))$ satisfies

$$(\mathbf{A} + [\![\mathbf{V} + \alpha \mathbf{u}^{②}(\alpha)]\!])\mathbf{u}(\alpha) = \lambda(\alpha)\mathbf{u}(\alpha) \quad (3.6a)$$

$$\mathbf{u}(\alpha)^\top \mathbf{u}(\alpha) = 1, \quad \mathbf{u}(\alpha) > 0, \quad (3.6b)$$

for all $\alpha \in [0, \alpha_1)$. By Perron-Fronbenius Theorem (10, p.27) we see that the eigenvalue $\lambda(\alpha)$ in (3.6a) is the minimal eigenvalue of $(\mathbf{A} + [\![\mathbf{V} + \alpha \mathbf{u}^{②}(\alpha)]\!])$ associated with the eigenvector $\mathbf{u}(\alpha) > 0$. Hence, the matrix $\bar{\mathbf{A}}(\alpha) \equiv \mathbf{A} + [\![\mathbf{V} + 3\alpha \mathbf{u}^{③}(\alpha)]\!] - \lambda(\alpha)\mathbf{I}_N$ is symmetric positive definitive, for all $\alpha \in [0, \alpha_1)$. Consequently, the matrix $\begin{bmatrix} \bar{\mathbf{A}}(\alpha) & \mathbf{u} \\ \mathbf{u}^\top & 0 \end{bmatrix}$ in (3.5) is nonsingular. By block elimination in Algorithm 2.1, the representation of $\mathbf{u}(\alpha)$ in (3.4) is easily obtained, for $\alpha \in [0, \alpha_1)$. Let $(\mathbf{u}(\alpha_1), \lambda(\alpha_1))$ be the limiting point of $(\mathbf{u}(\alpha), \lambda(\alpha))$, as $\alpha \to \alpha_1$. The point $(\mathbf{u}(\alpha_1), \lambda(\alpha_1))$ must satisfy (3.6a) with $\mathbf{u}(\alpha_1)^\top \mathbf{u}(\alpha_1) = 1$ and $\mathbf{u}(\alpha_1) \geq 0$. From Perron-Fronbenius Theorem again follows that $\mathbf{u}(\alpha_1) > 0$. By continuation method the IVP in (3.4) holds for all $\alpha \geq 0$.

It is easily seen that equations of (3.1) also form KKT (Karush-Kuhn-Tucker) equations of the optimization problem (3.3). Since the KKT point $(\mathbf{u}(\alpha), \lambda(\alpha))$ exists for all $\alpha \geq 0$ and $E_\alpha(\mathbf{u})$ is pseudoconvex, by the KKT sufficient condition (9, p.164) follows that $\mathbf{u}(\alpha)$ is a global minimizer of (3.3). The uniqueness of the global minimizer of (3.3) follows immediately from the uniqueness of the IVP in (3.4).

Furthermore, it is easy to show that $\frac{1}{\sqrt{N}}\mathbf{e}$ is the unique global minimizer of $\frac{1}{4}\mathbf{u}^{②\top}\mathbf{u}^{②}$. On the other hand, since

$$\frac{E_\alpha}{\alpha} = \frac{1}{2\alpha}(\mathbf{u}^\top \mathbf{A}\mathbf{u} + \mathbf{V}^\top \mathbf{u}^{②}) + \frac{1}{4}\mathbf{u}^{②\top}\mathbf{u}^{②} \to \frac{1}{4}\mathbf{u}^{②\top}\mathbf{u}^{②}, \text{ as } \alpha \to \infty,$$

this implies that the minimizer $\mathbf{u}(\alpha)$ converges to $\frac{1}{\sqrt{N}}\mathbf{e}$, as $\alpha \to \infty$.

Remark 3.1 *Recently, there have been extensive numerical and theoretical studies of the time independent GPE for ground states (8; 16; 18; 28; 32) and time-dependent GPE for dynamics (1; 5; 7; 15; 20) of a single-component*

BEC. Especially, in (28) the optimization problem (1.5a) *for* $m = 1$ *has been proven to have a unique global minimizer which converges to some limiting function, as* $\alpha \to \infty$. *Here in Theorem 3.1 we proved that the discretized optimization problem* (3.3) *has a unique global minimizer satisfying the IVP* (3.4) *and has a limit* $\frac{1}{\sqrt{N}}\mathbf{e}$, *as* $n \to \infty$. *Based on the result of* (3.4), *the solution curve of* (3.1) *can be parametrized by the natural parameter* α *and represented by* (3.5). *Thus, the continuation BSOR-Lanczos-Galerkin method developed in Section 2 can be used to compute all desired positive bound states of a single-component BEC.*

Corollary 3.1 *Let* $\mathbf{\Pi}_\theta$ *be a permutation such that*

$$(\mathcal{H}): \qquad \mathbf{\Pi}_\theta^\top \mathbf{A}\mathbf{\Pi}_\theta = \mathbf{A},\ \mathbf{\Pi}_\theta^\top [\![\mathbf{V}]\!]\mathbf{\Pi}_\theta = [\![\mathbf{V}]\!].$$

Then the global minimizer $\mathbf{u}(\alpha)$ *of* (3.3) *satisfies* $\mathbf{\Pi}_\theta(\mathbf{u}(\alpha)) = \mathbf{u}(\alpha)$, *for* $\alpha \geq 0$. *Moreover, it also holds* $\mathbf{\Pi}_\theta(\dot{\mathbf{u}}(\alpha)) = \dot{\mathbf{u}}(\alpha)$.

PROOF. By definition of $\mathbf{\Pi}_\theta$, it holds that

$$\mathbf{\Pi}_\theta \mathbf{u}(\alpha)^{\textcircled{r}} = (\mathbf{\Pi}_\theta \mathbf{u}(\alpha))^{\textcircled{r}},\ \ \mathbf{\Pi}_\theta [\![\mathbf{u}(\alpha)^{\textcircled{r}}]\!]\mathbf{\Pi}_\theta^\top = [\![(\mathbf{\Pi}_\theta \mathbf{u}(\alpha))^{\textcircled{r}}]\!]. \tag{3.7}$$

From Theorem 3.1, assumptions $(\mathcal{H})$ and (3.7) follows that $\mathbf{\Pi}_\theta(\mathbf{u}(\alpha))$ satisfies IVP in (3.4). Since the eigenvector $\mathbf{u}(0)$ (the ground state of (3.1) for $\alpha = 0$) corresponding to the minimal eigenvalue of $\mathbf{A}$ is invariant under $\mathbf{\Pi}_\theta$, i.e., $\mathbf{\Pi}_\theta(\mathbf{u}(0)) = \mathbf{u}(0)$. By the uniqueness of IVP it follows that $\mathbf{\Pi}_\theta(\mathbf{u}(\alpha)) = \mathbf{u}(\alpha)$, for $\alpha \geq 0$. Then last equation for the derivative of $\mathbf{u}(\alpha)$ holds by differentiating the equation $\mathbf{\Pi}_\theta(\mathbf{u}(\alpha)) = \mathbf{u}(\alpha)$ with respect to α, directly.

We now consider the NAEP of (2.1) for a multi-component BEC with $\mathbf{V}_j = \mathbf{V} \geq 0$, $\alpha_j = \alpha_0 \geq 0$ (fixed) and $\beta_{jk} = \beta_{kj} = \beta > 0$ (a parameter), $k \neq j$, $k, j = 1, \ldots, m$, i.e.,

$$\mathbf{A} + [\![\mathbf{V} + \alpha_0 \mathbf{u}_j^{\textcircled{2}} + \beta \sum_{k \neq j} \mathbf{u}_k^{\textcircled{2}}]\!]\mathbf{u}_j = \lambda_j \mathbf{u}_j, \tag{3.8a}$$

$$\mathbf{u}_j^\top \mathbf{u}_j = 1,\ j = 1, \ldots, m. \tag{3.8b}$$

The solution curve $\boldsymbol{\mathcal{C}}$ as in (2.8) corresponding to the NAEP (3.8) can be rewritten by

$$\boldsymbol{\mathcal{C}} = \{\mathbf{y}(s) = (\mathbf{x}^\top(s), \beta(s))^\top |\ \mathbf{G}(\mathbf{y}(\beta(s))) = 0\}, \tag{3.9}$$

where $\mathbf{x} = (\mathbf{u}_1^\top, \lambda_1, \ldots, \mathbf{u}_m^\top, \lambda_m)^\top$.

Theorem 3.2 *The solution curve* $\boldsymbol{\mathcal{C}}$ *as in* (3.9) *undergoes at least* $N - m$ *(*$N \gg m$*) bifurcation points at finite values* $\beta = \beta_q^* > 0$, $q = 1, \ldots, N - m$,

Moreover, the dimension of null space of $\mathbf{G}_{\mathbf{x}}(\mathbf{y}(\beta_q^*))$ *is at least* $m-1$, $q = 1,\ldots,N-m$.

PROOF. Since (3.8) has positive identical solutions $\mathbf{u}_1(\beta) = \cdots = \mathbf{u}_m(\beta)$, for β sufficiently small, the Jacobian matrix of (3.8) with respect to $\mathbf{x}$ is of the form

$$\mathbf{G}_{\mathbf{x}}(\mathbf{y}(\beta)) = \begin{bmatrix} \mathbf{B}_1 & \mathbf{E}_1 & \cdots & \mathbf{E}_1 \\ \mathbf{E}_1 & \mathbf{B}_1 & \ddots & \vdots \\ \vdots & \ddots & \ddots & \mathbf{E}_1 \\ \mathbf{E}_1 & \cdots & \mathbf{E}_1 & \mathbf{B}_1 \end{bmatrix}, \tag{3.10a}$$

where

$$\mathbf{B}_1 = \left[\begin{array}{c|c} \mathbf{A} + [\![\mathbf{V} + 3\alpha_0 \mathbf{u}_1^{②} + (m-1)\beta \mathbf{u}_1^{②}]\!] - \lambda_1 \mathbf{I} & \mathbf{u}_1 \\ \hline \mathbf{u}_1^{\top} & 0 \end{array}\right] \equiv \left[\begin{array}{c|c} \mathbf{A}_1 & \mathbf{u}_1 \\ \hline \mathbf{u}_1^{\top} & 0 \end{array}\right] \tag{3.10b}$$

and

$$\mathbf{E}_1 = \left[\begin{array}{c|c} 2\beta[\![\mathbf{u}_1^{②}]\!] & 0 \\ \hline 0 & 0 \end{array}\right]. \tag{3.10c}$$

For this situation, equations of (3.8) become one NAEP for $(\mathbf{u}_1, \lambda_1)$:

$$\mathbf{A}\mathbf{u}_1 + [\![\mathbf{V} + (\alpha_0 + (m-1)\beta)\mathbf{u}_1^{②}]\!]\mathbf{u}_1 = \lambda_1 \mathbf{u}_1, \quad \mathbf{u}_1^{\top}\mathbf{u}_1 = 1. \tag{3.11}$$

From (3.11) follows that the matrix $\mathbf{A}_1$ in (3.10b) is symmetric positive definitive, for β sufficiently small. Hence the matrix $\mathbf{B}_1$ in (3.10b) has N positive eigenvalues and one negative eigenvalue, and therefore, $\mathbf{G}_{\mathbf{x}}(\mathbf{y}(\beta))$ has Nm positive eigenvalues and m negative eigenvalues, for β sufficiently small.

From (3.10a), it is easily seen that

$$\mathbf{G}_{\mathbf{x}}(\mathbf{y}(\beta)) = \mathbf{I}_m \otimes \mathbf{B}_1 + \mathbf{C} \otimes \mathbf{E}_1, \text{ with } \mathbf{C} = \begin{bmatrix} 0 & 1 & \cdots & 1 \\ 1 & 0 & \ddots & \vdots \\ \vdots & \ddots & \ddots & 1 \\ 1 & \cdots & 1 & 0 \end{bmatrix}.$$

Here "$\otimes$" denotes the Kronecker product of two matrices. Using the fact that $\mathbf{C}$ has a simple eigenvalue $m-1$ and $m-1$ eigenvalues -1, there exist an

orthogonal matrix $\mathbf{Q}$ such that

$$\mathbf{Q}^\top \mathbf{C}\mathbf{Q} = \mathrm{diag}\{m-1, -1, \ldots, -1\}.$$

Multiplying $\mathbf{G}_{\mathbf{x}}(\mathbf{y}(\beta))$ in (3.10a) by $\mathbf{Q}\otimes\mathbf{I}_N$ from the right and by its transpose from the left, respectively, we obtain that

$$(\mathbf{Q}^\top \otimes \mathbf{I}_N)\mathbf{G}_{\mathbf{x}}(\mathbf{y}(\beta))(\mathbf{Q}\otimes\mathbf{I}_N) = \mathrm{diag}\{\mathbf{B}_1+(m-1)\mathbf{E}_1, \mathbf{B}_1-\mathbf{E}_1, \ldots, \mathbf{B}_1-\mathbf{E}_1\}. \tag{3.12}$$

From (3.10b), (3.10c) and (3.11) follow that the matrix $\mathbf{B}_1+(m-1)\mathbf{E}_1$ is nonsingular.

If we can show that $\mathbf{B}_1-\mathbf{E}_1$ has at least N negative eigenvalues ($N \gg m$), then it must exist at least $N-m$ finite $\beta_q^* > 0$ such that $\mathbf{G}_{\mathbf{x}}(\mathbf{y}(\beta_q^*))$ is singular. By Theorem 3.1 we also see that $\mathbf{x}$ can be parametrized by β, for all identical solutions $\mathbf{u}_1(\beta) = \cdots = \mathbf{u}_m(\beta)$. That is, the solution curve $\boldsymbol{\mathcal{C}}$ can not have a turning point at $\beta = \beta_q^*$. Hence, the solution curve $\boldsymbol{\mathcal{C}}$ must have bifurcation points at $\beta = \beta_q^* > 0$, $q = 1, \ldots, N-m$.

From Theorem 3.1 and (3.11) we have that $\lim_{\beta\to\infty} [\![\mathbf{u}_1(\beta)^{②}]\!] = \frac{1}{N}\mathbf{I}_N$, i.e., for any $\epsilon > 0$, there is a $\underline{\beta} > 0$ such that for all $\beta > \underline{\beta}$,

$$\frac{1}{N}\mathbf{I}_N - \epsilon < [\![\mathbf{u}_1(\beta)^{②}]\!] < \frac{1}{N}\mathbf{I}_N + \epsilon. \tag{3.13}$$

Let r be the maximal row sum of the off-diagonal elements of $\mathbf{A}$, $\bar{a}$ and $\underline{a}$ be the maximum and minimum of the diagonal elements of $\mathbf{A}+[\![\mathbf{V}]\!]$, respectively. By (3.13) and Gershgorin Theorem we have that

$$\underline{a} - r + (\alpha_0 + (m-1)\beta)(\frac{1}{N} - \epsilon) < \mu_i < \bar{a} + r + (\alpha_0 + (m-1)\beta)(\frac{1}{N} + \epsilon), \tag{3.14}$$

where μ_i is the eigenvalue of $\mathbf{A} + [\![\mathbf{V} + \alpha_0\mathbf{u}_1^{②} + (m-1)\beta\mathbf{u}_1^{②}]\!]$, for $i = 1, \ldots, N$, with $\mu_1 = \lambda_1$. This implies that

$$\mu_i - \lambda_1 < \bar{a} - \underline{a} + 2r + 2\epsilon(\alpha_0 + (m-1)\beta). \tag{3.15}$$

Rewrite $\mathbf{A}_1 - 2\beta[\![\mathbf{u}_1^{②}]\!]$ as in (3.10b) by

$$\mathbf{A}_1 - 2\beta[\![\mathbf{u}_1^{②}]\!] = \mathbf{A} + [\![\mathbf{V} + \alpha_0\mathbf{u}_1^{②} + (m-1)\beta\mathbf{u}_1^{②}]\!] - \lambda_1\mathbf{I} + 2(\alpha_0-\beta)[\![\mathbf{u}_1^{②}]\!]. \tag{3.16}$$

By (3.15) and Gershgorin Theorem again we show that all eigenvalues of $\mathbf{A}_1 - 2\beta[\![\mathbf{u}_1^{②}]\!]$ must be bounded by

$$b \equiv \bar{a} - \underline{a} + 3r + 2\epsilon(\alpha_0 + (m-1)\beta) + 2(\alpha_0-\beta)(\frac{1}{N} - \epsilon). \tag{3.17}$$

Since we can choose $\epsilon > 0$ sufficiently small and $\beta > 0$ sufficiently large so that the quantity b in (3.17) becomes negative, the N eigenvalues of $\mathbf{A}_1 - 2\beta[\![\mathbf{u}_1^{②}]\!]$, and thus of $\mathbf{B}_1 - \mathbf{E}_1$, become negative. This shows that the determinant of $\mathbf{G}_{\mathbf{x}}(\mathbf{y}(\beta))$ change signs at least $N - m$ times.

Finally, since $\mathbf{B}_1 - \mathbf{E}_1$ becomes singular at $\beta = \beta_q^*$, from equation (3.12) follows that $\dim \mathcal{N}(\mathbf{G}_{\mathbf{x}}(\mathbf{y}(\beta_q^*))) \geq m - 1$. We complete the proof.

Theorem 3.3 *Let $\mathbf{\Pi}_\theta$ be a permutation satisfy $(\mathcal{H})$ in Corollary 3.1 with $\mathbf{\Pi}_\theta^\top = \mathbf{\Pi}_\theta$. Then two identical bound states of NAEP (3.8) for a two-component BEC ($m = 2$) will bifurcate into two different positive bound states $\mathbf{u}_1$ and $\mathbf{u}_2$ at $\beta = \beta^* > 0$ with $\mathbf{\Pi}_\theta(\mathbf{u}_1) = \mathbf{u}_2$.*

Note that for the case $m \geq 3$, a theoretical proof is still open here. Numerical experiment shows that a symmetry breaking of m ground/bound states will occur at a finite value $\beta = \beta^*$.

PROOF. Let $\mathbf{G}(\mathbf{x}, \beta) = 0$ be defined in (2.6) and (2.7) corresponding to (3.8), and let $\mathbf{u}_1(\beta) = \mathbf{u}_2(\beta)$ be the identical solutions, for β sufficiently small. From (3.10) and (3.5) by replacing $\mathbf{u}(\alpha_0 + \beta)$ by $\mathbf{u}_1(\beta)$, we have

$$\left[\, \mathbf{G}_{\mathbf{x}} \middle| \mathbf{G}_\beta \,\right] \begin{bmatrix} \dot{\mathbf{u}}_1(\beta) \\ -\dot{\lambda}_1(\beta) \\ \dot{\mathbf{u}}_1(\beta) \\ -\dot{\lambda}_1(\beta) \\ 1 \end{bmatrix} = \left[\begin{array}{cc|c} \multicolumn{2}{c|}{\multirow{2}{*}{$\mathbf{B}_1 \;\; \mathbf{E}_1$}} & \mathbf{u}_1^{③} \\ & & 0 \\ \hline \multicolumn{2}{c|}{\multirow{2}{*}{$\mathbf{E}_1 \;\; \mathbf{B}_1$}} & \mathbf{u}_1^{③} \\ & & 0 \end{array}\right] \begin{bmatrix} \dot{\mathbf{u}}_1(\beta) \\ -\dot{\lambda}_1(\beta) \\ \dot{\mathbf{u}}_1(\beta) \\ -\dot{\lambda}_1(\beta) \\ 1 \end{bmatrix} = 0. \tag{3.18}$$

Then $\bar{\mathbf{u}}_1 \equiv (\dot{\mathbf{u}}_1^\top(\beta), -\dot{\lambda}_1(\beta), \dot{\mathbf{u}}_1^\top(\beta), -\dot{\lambda}_1(\beta), 1)^\top$ is a natural tangent vector of the solution curve $\boldsymbol{\mathcal{C}}$ of (3.9) for the identical solutions. Since by Corollary 3.1 and assumption $(\mathcal{H})$ we have $\mathbf{\Pi}_\theta \mathbf{A} \mathbf{\Pi}_\theta = \mathbf{A}$ and $\mathbf{\Pi}_\theta \mathbf{u}_1 = \mathbf{u}_1$ for β sufficiently small, the matrix $\widehat{\mathbf{A}}_1 \equiv \mathbf{A}_1 - 2\beta[\![\mathbf{u}_1^{②}]\!]$ satisfies $\mathbf{\Pi}_\theta \widehat{\mathbf{A}}_1 \mathbf{\Pi}_\theta = \widehat{\mathbf{A}}_1$, where $\mathbf{A}_1$ is defined in (3.10b). Hence, the eigenvectors, say $\boldsymbol{\xi}_1$ of $\widehat{\mathbf{A}}_1$ corresponding to the eigenvalues in increasing order are alternating symmetric (i.e., $\mathbf{\Pi}_\theta \boldsymbol{\xi}_1 = \boldsymbol{\xi}_1$) and anti-symmetric (i.e., $\mathbf{\Pi}_\theta \boldsymbol{\xi}_1 = -\boldsymbol{\xi}_1$). In fact, by the definition of $\widehat{\mathbf{A}}_1$ one can show that $\widehat{\mathbf{A}}_1 \mathbf{u}_1 = 0$ for $\beta = \alpha_0$, but $\mathbf{B}_1 - \mathbf{E}_1$ is nonsingular for $\beta = \alpha_0$. Therefore, there is a $\beta^* > \alpha_0$ and an anti-symmetric null vector $\boldsymbol{\xi}_1 \in \mathbb{R}^N$ of $\widehat{\mathbf{A}}_1$ at $\beta = \beta^*$ as in Theorem 3.2. That is,

$$(\mathbf{B}_1 - \mathbf{E}_1) \begin{bmatrix} \boldsymbol{\xi}_1 \\ 0 \end{bmatrix} = 0, \quad \text{for } \beta = \beta^* > 0. \tag{3.19}$$

Consequently, it holds

$$\left[\,\mathbf{G}_{\mathbf{x}}\middle|\mathbf{G}_{\beta}\,\right]\begin{bmatrix}\boldsymbol{\xi}_1\\0\\-\boldsymbol{\xi}_1\\0\\0\end{bmatrix}=0. \tag{3.20}$$

Furthermore, from Corollary 3.1 it holds that $\dot{\mathbf{u}}_1^{\top}\boldsymbol{\xi}_1=0$ because $\dot{\mathbf{u}}_1$ is symmetric, therefore, the vector $\bar{\boldsymbol{\xi}_1}\equiv(\boldsymbol{\xi}_1^{\top},0,-\boldsymbol{\xi}_1^{\top},0,0)^{\top}$ and $\bar{\mathbf{u}}_1$ are mutually perpendicular at the bifurcation point $\beta=\beta^*$. This coincides with case (I) of (2.16). Hence the vector $\bar{\boldsymbol{\xi}}$ forms another tangent vector of $\boldsymbol{\mathcal{C}}$. Since $\boldsymbol{\Pi}_{\theta}\boldsymbol{\xi}_1=-\boldsymbol{\xi}_1$, we let

$$\mathbf{y}_1=\begin{bmatrix}\mathbf{u}_1+\epsilon\boldsymbol{\xi}_1\\\lambda_1\\\mathbf{u}_1-\epsilon\boldsymbol{\xi}_1\\\lambda_1\\\beta\end{bmatrix}\equiv\begin{bmatrix}\mathbf{v}_1\\\lambda_1\\\boldsymbol{\Pi}_{\theta}\mathbf{v}_1\\\lambda_1\\\beta\end{bmatrix} \tag{3.21}$$

be the prediction vector for the Newton correction (2.10), where ϵ is sufficiently small and $\beta\approx\beta^*$. From (3.7) the linear bordered system of (2.10) becomes

$$\left[\begin{array}{c|c|c}\bar{\mathbf{B}}_1&\bar{\mathbf{E}}_1&\mathbf{v}_1\circ(\boldsymbol{\Pi}_{\theta}\mathbf{v}_1)^{②}\\&&0\\\hline\bar{\mathbf{E}}_1&\bar{\boldsymbol{\Pi}}_{\theta}\bar{\mathbf{B}}_1\bar{\boldsymbol{\Pi}}_{\theta}&(\boldsymbol{\Pi}_{\theta}\mathbf{v}_1)\circ\mathbf{v}_1^{②}\\&&0\\\hline\boldsymbol{\xi}_1^{\top},\ 0&-\boldsymbol{\xi}_1^{\top},\ 0&0\end{array}\right]\left[\begin{array}{c}\boldsymbol{\delta}_1\\\hline\hat{\boldsymbol{\delta}}_1\\\hline\kappa\end{array}\right]=\left[\begin{array}{c}-\mathbf{G}(\mathbf{y}_1)\\0\\\hline-\boldsymbol{\Pi}_{\theta}\mathbf{G}(\mathbf{y}_1)\\0\\\hline0\end{array}\right], \tag{3.22}$$

where $\bar{\boldsymbol{\Pi}}_{\theta}=\begin{bmatrix}\boldsymbol{\Pi}_{\theta}&0\\0&1\end{bmatrix}$, $\boldsymbol{\delta},\ \hat{\boldsymbol{\delta}}_1\in\mathbb{R}^{N+1}$,

$$\bar{\mathbf{B}}_1=\left[\begin{array}{c|c}\mathbf{A}+[\![\mathbf{V}+3\alpha_0\mathbf{v}_1^{②}]\!]+\beta\boldsymbol{\Pi}_{\theta}[\![\mathbf{v}_1^{②}]\!]\boldsymbol{\Pi}_{\theta}-\lambda_1\mathbf{I}&\mathbf{v}_1\\\hline\mathbf{v}^{\top}&0\end{array}\right], \tag{3.23a}$$

$$\bar{\mathbf{E}}_1=\left[\begin{array}{c|c}[\![2\beta\mathbf{v}_1\circ\boldsymbol{\Pi}_{\theta}\mathbf{v}_1]\!]&0\\\hline0^{\top}&0\end{array}\right] \tag{3.23b}$$

and

$$\mathbf{G}(\mathbf{y}_1) = \mathbf{A}\mathbf{v}_1 + \mathbf{V} \circ \mathbf{v}_1 + \alpha_0 \mathbf{v}_1^{③} + \beta(\mathbf{\Pi}_\theta \mathbf{v}_1)^{②} \circ \mathbf{v}_1 - \lambda_1 \mathbf{v}_1. \tag{3.23c}$$

Expanding (3.22), we get equations

$$\bar{\mathbf{B}}_1 \boldsymbol{\delta}_1 + \bar{\mathbf{E}}_1 \hat{\boldsymbol{\delta}}_1 = \mathbf{g}_1, \tag{3.24a}$$

$$\bar{\mathbf{E}}_1 \boldsymbol{\delta}_1 + \bar{\mathbf{\Pi}}_\theta \bar{\mathbf{B}}_1 \bar{\mathbf{\Pi}}_\theta \hat{\boldsymbol{\delta}}_1 = \bar{\mathbf{\Pi}}_\theta \mathbf{g}_1, \tag{3.24b}$$

where

$$\mathbf{g}_1 = \begin{bmatrix} -\mathbf{G}(\mathbf{y}_1) \\ 0 \end{bmatrix} - \kappa \begin{bmatrix} \mathbf{v}_1 \circ (\mathbf{\Pi}_\theta \mathbf{v}_1)^{②} \\ 0 \end{bmatrix}.$$

Multiplying (3.24b) by $\bar{\mathbf{\Pi}}_\theta$ from the left and using the fact that $\bar{\mathbf{\Pi}}_\theta \bar{\mathbf{E}}_1 = \bar{\mathbf{E}}_1 \bar{\mathbf{\Pi}}_\theta$ we obtain

$$(\bar{\mathbf{B}}_1 - \bar{\mathbf{E}}_1 \bar{\mathbf{\Pi}}_\theta)(\boldsymbol{\delta}_1 - \bar{\mathbf{\Pi}}_\theta \hat{\boldsymbol{\delta}}_1) = 0. \tag{3.25}$$

Since the Jacobian matrix in (3.22) is nonsingular for some $\beta \approx \beta^*$ and $\beta \neq \beta^*$, the matrix $(\bar{\mathbf{B}}_1 - \bar{\mathbf{E}}_1 \bar{\mathbf{\Pi}}_\theta)$ is nonsingular for $\beta \approx \beta^*$. From (3.25) follows that $\hat{\boldsymbol{\delta}}_1 = \bar{\mathbf{\Pi}}_\theta \boldsymbol{\delta}_1$. This implies that starting with $\mathbf{y}_1$ given in (3.21) we always have a symmetric correction by each Newton step in (3.22), i.e.,

$$\mathbf{y}_{l+1} = \mathbf{y}_l + \begin{bmatrix} \boldsymbol{\delta}_1 \\ \bar{\mathbf{\Pi}}_\theta \boldsymbol{\delta}_1 \\ \kappa \end{bmatrix}, l = 1, 2, \ldots. \tag{3.26}$$

If ϵ in (3.21) is chosen sufficiently small, then the Newton correction (3.26) will converge to positive bound state solutions $\begin{bmatrix} \mathbf{u}_1 \\ \lambda_1 \end{bmatrix}$ and $\begin{bmatrix} \mathbf{u}_2 \\ \lambda_1 \end{bmatrix}$ lying on the solution curve $\boldsymbol{\mathcal{C}}$ of (3.8) ($m = 2$) with $\mathbf{u}_2 = \mathbf{\Pi}_\theta(\mathbf{u}_1)$.

Remark 3.2 *The equation* (3.19) *in the proof of Theorem 3.3 shows that if the β^* is the first singular point which we undergo by the path following, then two identical ground states will bifurcate into two different ground states $\mathbf{u}_1$ and $\mathbf{u}_2$ with $\mathbf{u}_2 = \mathbf{\Pi}_\theta(\mathbf{u}_1)$.*

4 Numerical Examples

In Section 2 we developed a continuation BSOR-Lanczos-Galerkin method which can be utilized to compute possibly all positive bound states of a multi-

component BEC. The solution curve of (2.6) is traced by the proposed continuation method implemented by a MATLAB V6.5 (16 digits) on an Intel Pentium 4 Processor. The tolerance of each step in Newton correction (2.10) is chosen to be $Tol = 10^{-8}$.

In physical applications and numerical simulations we first study the bifurcation of the NAEP (2.1) under assumptions (2.4) in the following four cases for $m = 2$.

Case 1: $\alpha_1 = \alpha_2 \equiv \alpha_0$ (i.e., $\mu_0 = 0$) fixed, $\beta_{12} = \beta_{21} := \beta > 0$ (parameter),
Case 2: $\beta_{12} = \beta_{21} \equiv \beta_0$ (i.e., $\nu_0 = 0$) fixed, $\alpha_1 = \alpha_2 := \alpha > 0$ (parameter),
Case 3: $\alpha_1 = \alpha_2 := \alpha_0 + \mu_0 p$, $\beta_{12} = \beta_{21} := \beta_0 + \nu_0 p$, $\mu_0 < \nu_0$, $p > 0$ (parameter),
Case 4: $\alpha_1 = \alpha_2 := \alpha_0 + \mu_0 p$, $\beta_{12} = \beta_{21} := \beta_0 + \nu_0 p$, $\mu_0 > \nu_0$, $p > 0$ (parameter).

Example 4.1 Let $m = 2$, $\Omega = [-5, 5] \times [-4.8, 4.8]$, $\mathbf{V}_1 = \mathbf{V}_2 = x^2 + y^2$. The uniform mesh size h of the grid domain Ω_h is chosen by $h = 0.1$. Let $\mathbf{\Pi}_\theta$ denote the symmetric reflection of Ω_h with respect to y-axis, i.e., $\mathbf{\Pi}_\theta(\Omega_h) = \Omega_h$. Furthermore, it holds that $\mathbf{\Pi}_\theta^\top \mathbf{A} \mathbf{\Pi}_\theta = \mathbf{A}$ and $\mathbf{\Pi}_\theta^\top [\![\mathbf{V}_1]\!] \mathbf{\Pi}_\theta = [\![\mathbf{V}_1]\!]$, where $\mathbf{A}$ is the discretized approximation of $-\nabla^2$ by the standard central finite difference.

In Figure 4.0 we plot the bifurcation curves of the NAEP (2.1) for $\alpha \in (0, 28)$ and $\beta \in (0, 15)$ in solid lines. Then along the 4 different dot line we compute the bifurcation diagrams of (2.1) of the following 4 cases.

Case 1. For $\alpha_0 = 2$, $\beta_{12} = \beta_{21} = \beta > 0$: In Figures 4.1(a)(b) we plot the bifurcation diagrams of positive bound states of NAEP (2.1) versus the repulsive scattering length β, for $\beta \in (0, 28)$ and $\beta \in (93, 125)$, respectively. Here the nodal domains of positive bound state solutions are attached near the solution curves. The NAEP undergoes the bifurcation at singular points $\beta_1^* = 6.56$, $\beta_2^* = 11.55$, $\beta_3^* = 14.34$, $\beta_4^* = 24.53$, $\beta_5^* = 95.48$, $\beta_6^* = 96.84$, $\beta_7^* = 98.43$, $\beta_8^* = 113.66$, $\beta_9^* = 117.27$, respectively. Two new born positive bound solutions $\mathbf{u}_1$ and $\mathbf{u}_2$ satisfy $\mathbf{\Pi}_\theta(\mathbf{u}_1) = \mathbf{u}_2$.

Furthermore, in Figures 4.1(c) and 4.1(d) we plot the solution curves of eigenvalues and the associated solution curves of energy versus β, for $\beta \in (0, 28)$ and $\beta \in (93, 125)$, respectively. In addition, the level sets of two bound state solutions are attached near the solution curves of energy.

From Figures 4.1 and Theorem 3.3 we observe that for $0 \le \beta < \beta_1^*$, the NAEP (2.1) has only identical ground state solutions, and undergoes a bifurcation point at $\beta = \beta_1^*$, so that the ground state solutions begin to separate for $\beta > \beta_1^*$. Since $\beta > 0$ is a repulsive scattering length, it is expected that the ground state solutions of (2.1) should be little by little mutually separated when this bifurcation branch is traced with continually increasing β. The structure of the phase separation will finally reach a stage of totally disjoint nodal domains, when β approaches to 10^5. Next, we come back to the bifurcation point β_1^* on the primal stalk and trace the solution

curve with identical bound state solutions for $\beta > \beta_1^*$. By path following, we will undergo a sequence of bifurcation points $\{\beta_i^*\}_{i=2}^9$ on the primal stalk. For each bifurcation branch at β_i^*, if we trace the solution curve with $\beta > \beta_i^*$, a new structure of positive bound state solutions will be found.

Case 2. For $\beta_0 = 15$, $\alpha_1 = \alpha_2 = \alpha > 0$: In Figure 4.2(a) we plot the bifurcation diagram of positive bound state solutions of NAEP (2.1) for $\alpha \in (0, 15)$. We see that the NAEP undergoes the bifurcation at singular points $\alpha_1^* = 10.69$, $\alpha_2^* = 5.16$, $\alpha_3^* = 2.71$. In Figure 4.2(b) we plot the associated solution curves of eigenvalues and energy versus α, for $\alpha \in (0, 15)$. Note that here we follow the solution curves of NAEP along α decreasingly.

From Figures 4.2 we observe that the NAEP (2.1) has identical ground state solutions. For $\alpha_1^* < \alpha \leq 15$ and undergoes a bifurcation point at $\alpha = \alpha_1^*$ so that the ground state solutions separate into two solutions symmetrized with respect to $\mathbf{\Pi}_\theta$. Then, we follow the solution curve on the primal stalk for $\alpha < \alpha_1^*$ and we will undergo a sequence of bifurcation points $\{\alpha_i^*\}_{i=2}^3$. For each bifurcation branch at α_i^*, if we trace the solution curves with $\alpha < \alpha_i^*$, a new structure of positive bound state solutions will be found.

In light of the bifurcation curves in Figures 4.0, Figures 4.1(a) and 4.2(a) we observe that the bifurcation diagram of case 2 for increasing α is somewhat like a reverse diagram of the bifurcation diagram of case 1 for increasing β.

Case 3. For $\alpha_0 = 0$, $\beta_0 = 0$, $\mu_0 = 0.1$ and $\nu_0 = 1$: In Figure 4.3(a) and 4.3(b) we plot the bifurcation diagram of NAEP (2.1), and the associated solution curves of eigenvalues as well as energy, respectively, versus p, for $p \in (0, 28)$. The NAEP undergoes the bifurcation at $p_1^* = 5.16$, $p_2^* = 10.48$, $p_3^* = 13.84$, $p_4^* = 25.05$.

In light of the bifurcation curves of NAEP in Figure 4.0 we observe that the bifurcation diagram of case 3 is quite similar to that of case 1. Only difference is that the bifurcation point of case 3 occurs later then that of case 1.

Case 4. For $\alpha_0 = 0$, $\beta_0 = 0$, $\mu_0 = 1$ and $\nu_0 = 0.5$: In Figure 4.4 we plot the bifurcation diagram of NAEP (2.1), for $p \in (0, 15)$ and show that there is no bifurcation for this trivial case.

Example 4.2 Let $m = 3$, $\Omega = [-5, 5] \times [-4.8, 4.8]$, $\mathbf{V}_1 = \mathbf{V}_2 = \mathbf{V}_3 = x^2 + y^2$. The mesh size is the same as in Example 4.1. We consider the case of that $\alpha_1 = \alpha_2 = \alpha_3 = 0.1$, $\beta_{kj} = \beta > 0$ (parameter), for $k \neq j$, $k, j = 1, 2, 3$. Solutions and bifurcations of NAEP (2.1) are computed by BSOR-Lanczos-Galerkin algorithm. Here by path following, we follow the solution curve at each bifurcation point only along one trial tangent vector obtained in Algorithm 2.4. Slight different from Example 4.1, for convenience and for simplicity, we omit the bifurcation diagram but plot the solution curve of eigenvalues for $\beta \in (8.7, 51)$ and attach the nodal domains of positive bound state solutions near the corresponding eigenvalues in Figure 4.5. Furthermore,

we plot the solution curve of energy for $\beta \in (8.7, 51)$ and attach the level sets of positive bound states near the corresponding energy in Figure 4.6.

5 Conclusions

In this paper, we developed a continuation BSOR-Lanczos-Galerkin method for the computation of positive bound states of a multi-component BEC. The bifurcation diagram of positive eigenvectors/eigenvalues of NAEP and the associated energy functional of the time-independent CGPEs is traced by the proposed continuation method. Numerical experience shows that our method performs reliably and efficiently. Different from NGF, TSSP and GSI methods for the computation of the ground states of a multi-component BEC only, the continuation method is proposed from the viewpoint of a nonlinear eigenvalue approach, which can be used for computing all possible positive bound states of a multi-component BEC. We proved that a phase separation of m ground/bound states will occur at a finite value of the repulsive scattering length. For a two-component BEC, we also proved that two identical ground/bound states will bifurcate into different $\mathbf{\Pi}_\theta$-symmetry ground/bound states. In the future, we are interested in proving the existence of the $\mathbf{\Pi}_\theta$-symmetry phase separation for the ground/bound states of a multi-component BEC ($m \geq 3$).

References

[1] A. Aftalion and Q. Du. Vortices in a rotating Bose-Einstein condensate: Critical angular velocities and energy diagrams in the Thomas-Fermi regime. *Phys. Rev. A*, 64:063603, 2001.

[2] E.L. Allgower and K. Georg. Numerical path following. In: *Handbook of Nemerical Analysis*, North-Holland, editors, P. G. Ciarlet and J. L. Lions, 5:3–207, 1997.

[3] P. Ao and S. T. Chui. Binary Bose-Einstein condensate mixtures in weakly and strongly segregated phases. *Phys. Rev. A*, 58:4836–4840, 1998.

[4] W. Z. Bao. Ground states and dynamics of multi-component Bose-Einstein condensates. *SIAM Multiscale Modeling and Simulation*, to appear.

[5] W. Z. Bao and Q. Du. Computing the ground state solution of Bose-Einstein condensates by a normalized gradient flow. *SIAM J. Sci. Comp.*, to appear.

[6] W. Z. Bao and D. Jaksch. An explicit unconditionally stable numerical methods for solving damped nonlinear Schrödinger equations with a focusing nonlinearity. *SIAM J. Numer. Anal*, 41(4):1406–1426, 2003.

[7] W. Z. Bao, D. Jaksch, and P. A. Markowich. Numerical solution of the Gross-Pitaevskii equation for Bose-Einstein condensation. *J. Comp. Phys.*, 187:318–342, 2003.

[8] W. Z. Bao and W. J. Tang. Ground state solution of trapped interacting Bose-Einstein condensate by directly minimizing the energy functional. *J. Comp. Phys.*, 187:230–254, 2003.

[9] M. S. Bazaraa, H. D. Sherali, and C. M. Shetty. *Nonlinear programming: theory and algorithms*. Wiley, New York, 2 edition, 1993.

[10] A. Berman and R. J. Plemmons. *Nonnegative matrices in the mathematical sciences*. Academic Press, New York, 1979.

[11] M. Berry. Large scale singular value computations. *Internat. J. Supercomputer Appl.*, 6(1):13–49, 1992.

[12] T. F. Chan. Deflation techniques and block-elimination algorithm for solving bordered singular systems. *SIAM J. Sci. Stat. Comp.*, 5:121–134, 1984.

[13] S. M. Chang, C. S. Lin, T. C. Lin, and W. W. Lin. Segregated nodal domains of two-dimensional multispecies Bose-Einstein Condensates. *Physica D*, 196:341–361, 2004.

[14] S. M. Chang, W. W. Lin, and S. F. Shieh. Gauss-seidel-type methods for energy states of a multi-component Bose-Einstein Condensate. *J. Comp. Phys.*, 202:367–390, 2005.

[15] M. L. Chiofalo, S. Succi, and M. P. Tosi. Ground state of trapped interacting Bose-Einstein condensates by an explicit imaginary-time algorithm. *Phys. Rev. E*, 62:7438–7444, 2000.

[16] Y. S. Choi, J. Javanainen, I. Koltracht, M Koštrun, P. J. Mckenna, and N. Savytska. A fast algorithm for the solution of the time-independent Gross-Pitaevskii equation. *J. Comp. Phys.*, to appear.

[17] B. D. Davidson. Large-scale continuation and numerical bifurcation for partial differential equations. *SIAM J. Numer. Anal.*, 34:2008–2027, 1997.

[18] R. J. Dodd. Approximate solutions of the nonlinear Schrödinger equation for ground and excited states of Bose-Einstein condensates. *J. Res. Natl. Inst. Stan.*, 101:545–552, 1996.

[19] B. D. Esry and C. H. Greene. Spontaneous spatial symmetry breaking in two-component Bose-Einstein condensates. *Phys. Rev. A*, 59:1457–1460, 1999.

[20] B. D. Esry, C. H. Greene, J. P. Burke Jr, and J. L. Bohn. Hartree-Fock theory for double condensates. *Phys. Rev. Lett.*, 78:3594–3597, 1997.

[21] W. Govaerts. Stable solvers and block elimination for bordered systems. *SIAM J. Matrix Anal. Appl.*, 12:469–483, 1991.

[22] W. Govaerts and J.D. Pryce. Mixed block elimination for linear systems with wider borders. *IMA J. Numer. Anal.*, 13:161–180, 1993.

[23] Willy J. F. Govaerts. *Numerical Methods for Bifurcations of Dynamical Equilibria Computations*. SIAM, Philadelphia, 2000.

[24] G. H. Golub and C. F. Van Loan. *Matrix Computations*. Second edition, Johns Hopkins University Press, Baltimore, MD, 1989.

[25] S. Gutpa, Z. Hadzibabic, M. W. Zwierlein, C. A. Stan, K. Dieckmann, C. H. Schunck, E. G. M. van Kempen, B. J. Verhaar, and W. Ketterle. Radio-frequency spectroscopy of Ultracold Fermions. *Science*, 300:1723–1726, 2003.

[26] D. S. Hall, M. R. Matthews, J. R. Ensher, C. E. Wieman, and E. A. Cornell. Dynamics of component separation in a binary mixture of Bose-Einstein condensates. *Phys. Rev. Lett.*, 81:1539–1542, 1998.

[27] H. B. Keller. *Lectures on Numerical Methods in Bifurcation Problems*. Springer-Verlag, Berlin, 1987.

[28] E. H. Lieb, R. Seiringer, and J. Yngvason. Bosons in a trap: a rigorous derivation of Gross-Pitaevskii energy functional. *Phys. Rev. A*, 61:043602, 2000.

[29] C. J. Myatt, E. A. Burt, R. W. Ghrist, E. A. Cornell, and C. E. Wieman. Production of two overlapping Bose-Einstein condensates by sympathetic cooling. *Phys. Rev. Lett.*, 78:586–589, 1997.

[30] B. N. Parlett. A new look at the Lanczos algorithm for solving symmetric systems of linear equations. *Lin. Alg. Appl.*, 29:323–346, 1980.

[31] Y. Saad. On the Lanczos method for solving symmetric linear systems with several right-hand-sides. *Math. Comp.*, 48:651–662, 1987.

[32] B. I. Schneider and D. K. Feder. Numerical approach to the ground and excited states of a Bose-Einstein condensated gas confined in a completely anisotropic trap. *Phys. Rev. A*, 59:2233–2242, 1999.

[33] J. Stoer and R. Bulirsch. *Introduction to Numerical Analysis*. Springer-Verlag, Berlin, 2 edition, 1991.

[34] L. T. Watson, S. C. Billups, and A. P. Morgan. HOMPACK: A suite of codes for globally convergent homotopy algorithms. *ACM Trans. Math. Software*, 13:281–310, 1987.

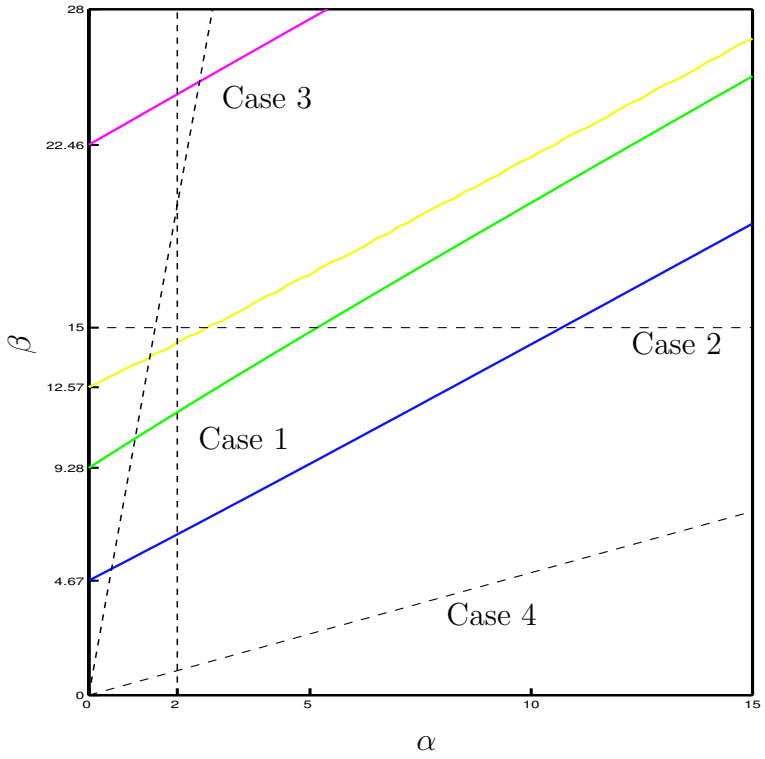

Figure 4.0. Bifurcation curves of NAEP.

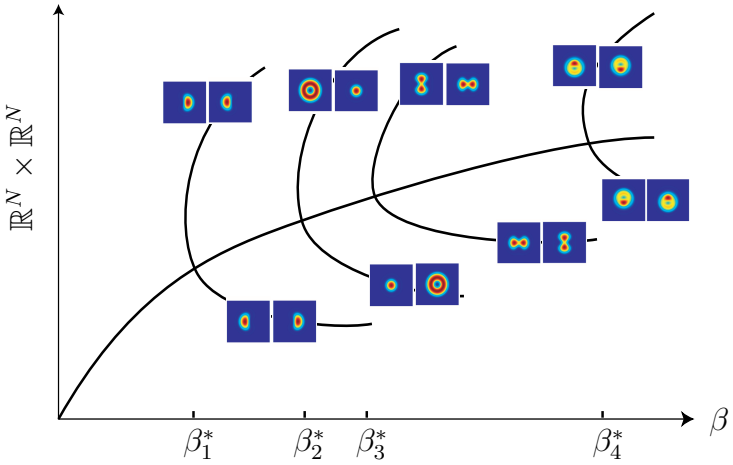

Figure 4.1(a). Bifurcation diagram of NAEP for $\alpha_0 = 2, \beta \in (0, 28)$.

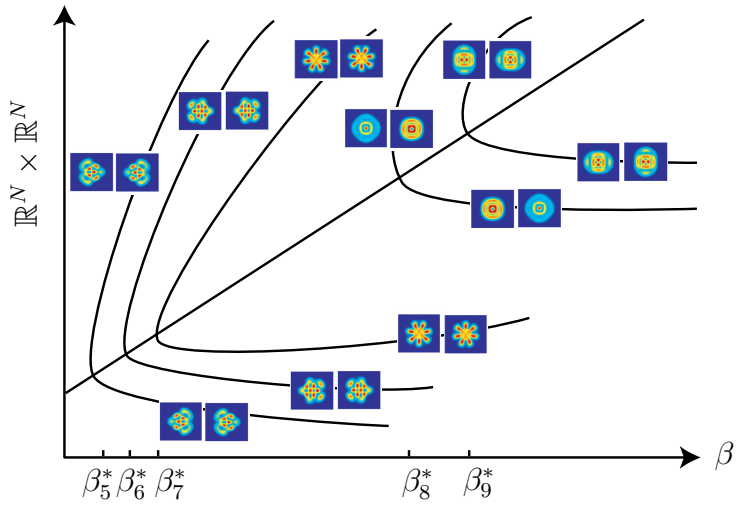

Figure 4.1(b). Bifurcation diagram of NAEP for $\alpha_0 = 2, \beta \in (93, 125)$.

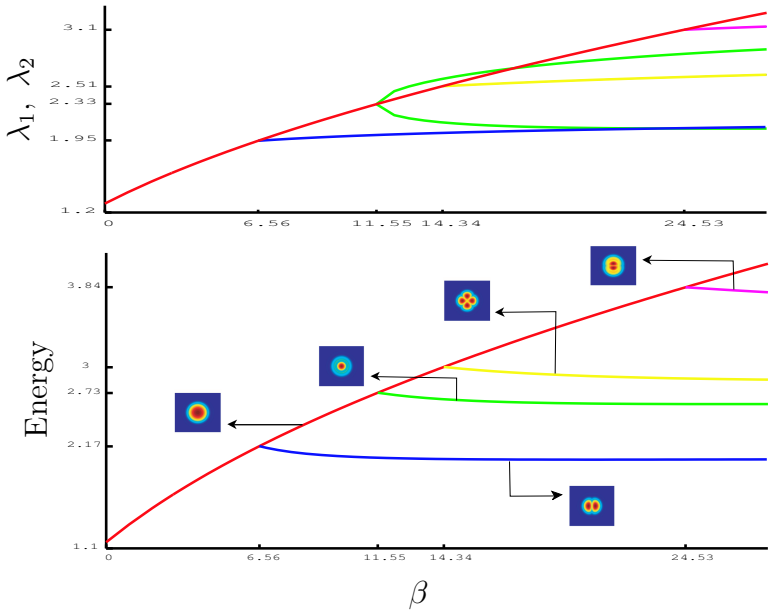

Figure 4.1(c). Solution curve of eigenvalues and energy for $\alpha_0 = 2, \beta \in (0, 28)$.

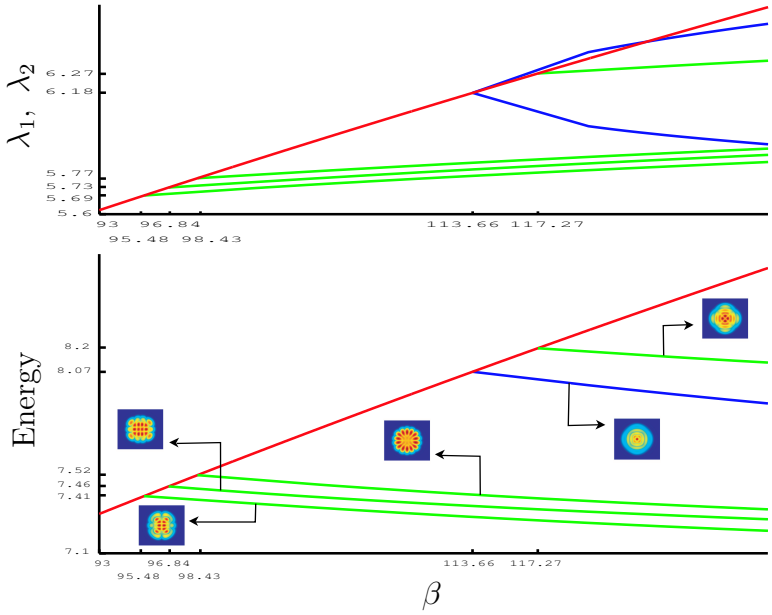

Figure 4.1(d). Solution curve of eigenvalues and energy for $\alpha_0 = 2, \beta \in (93, 125)$.

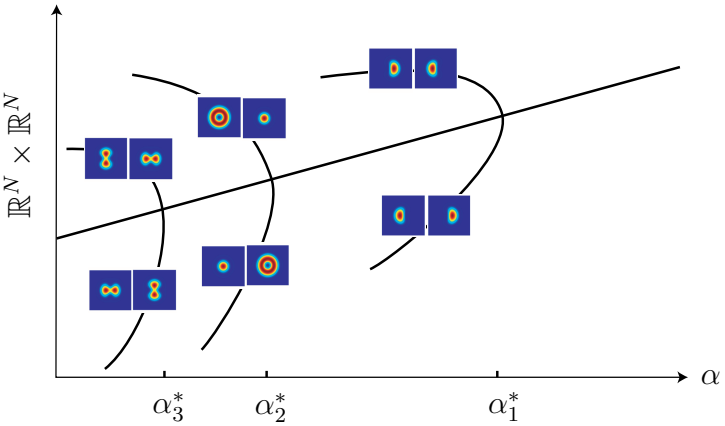

Figure 4.2(a). Bifurcation diagram of NAEP for $\beta_0 = 15, \alpha \in (0, 15)$.

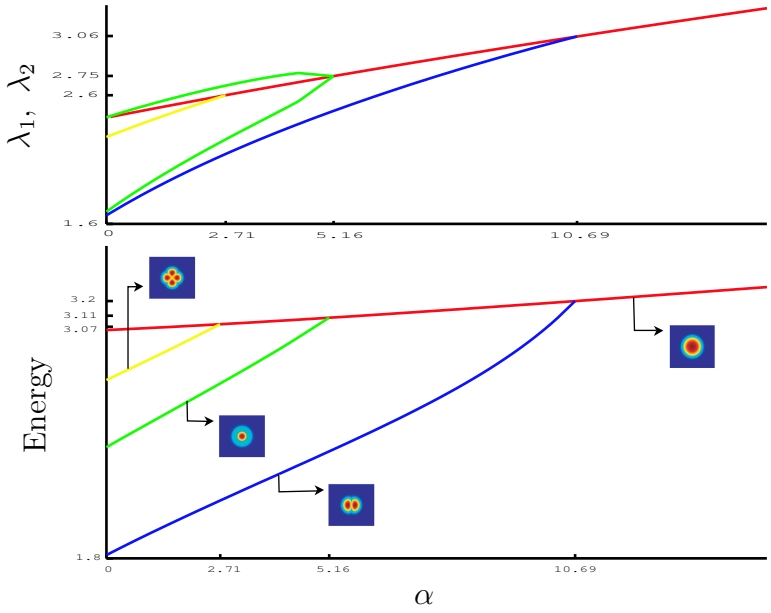

Figure 4.2(b). Solution curve of eigenvalues and energy for $\beta_0 = 15, \alpha \in (0, 15)$.

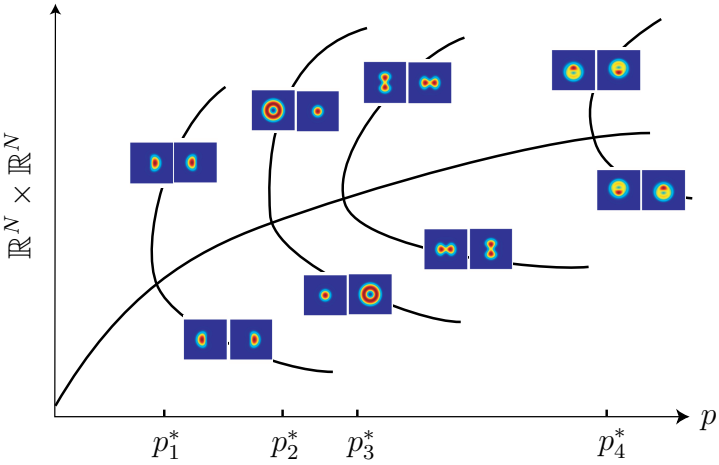

Figure 4.3(a). Bifurcation diagram of NAEP for $\alpha_0 = 0$, $\beta_0 = 0$, $\mu_0 = 0.1$ and $\nu_0 = 1$.

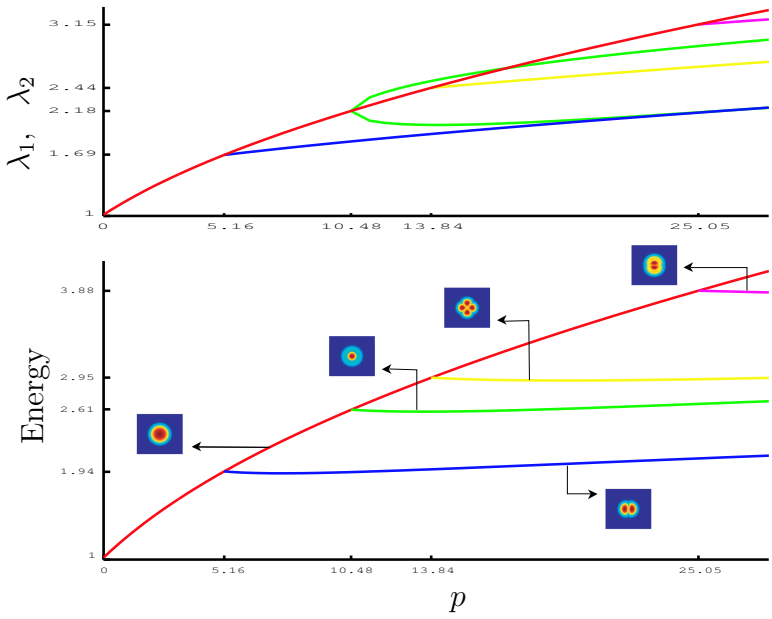

Figure 4.3(b). Solution curve of eigenvalues and energy for $\alpha_0 = 0, \beta_0 = 0, \mu_0 = 0.1$ and $\nu_0 = 1$.

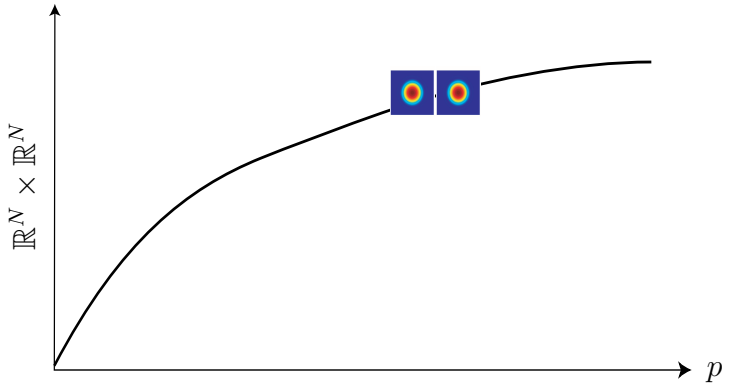

Figure 4.4. Bifurcation diagram of NAEP for $\alpha_0 = 0$, $\beta_0 = 0$, $\mu_0 = 1$ and $\nu_0 = 0.5$.

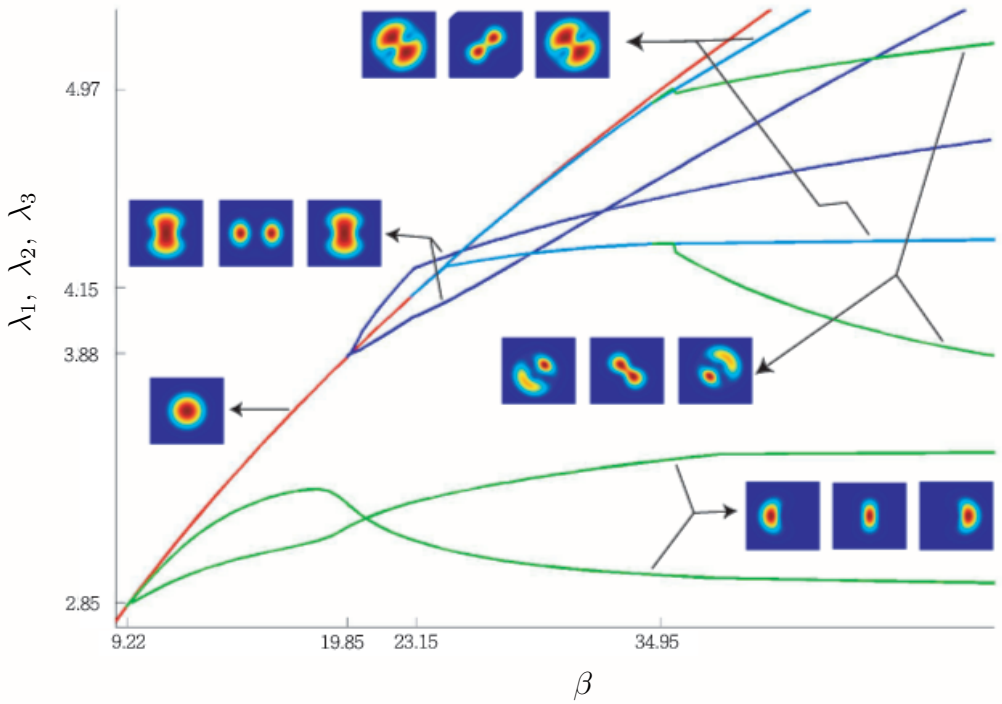

Figure 4.5. $m = 3$. Solution curve of eigenvalues versus β for $\beta \in (8.7, 51)$.

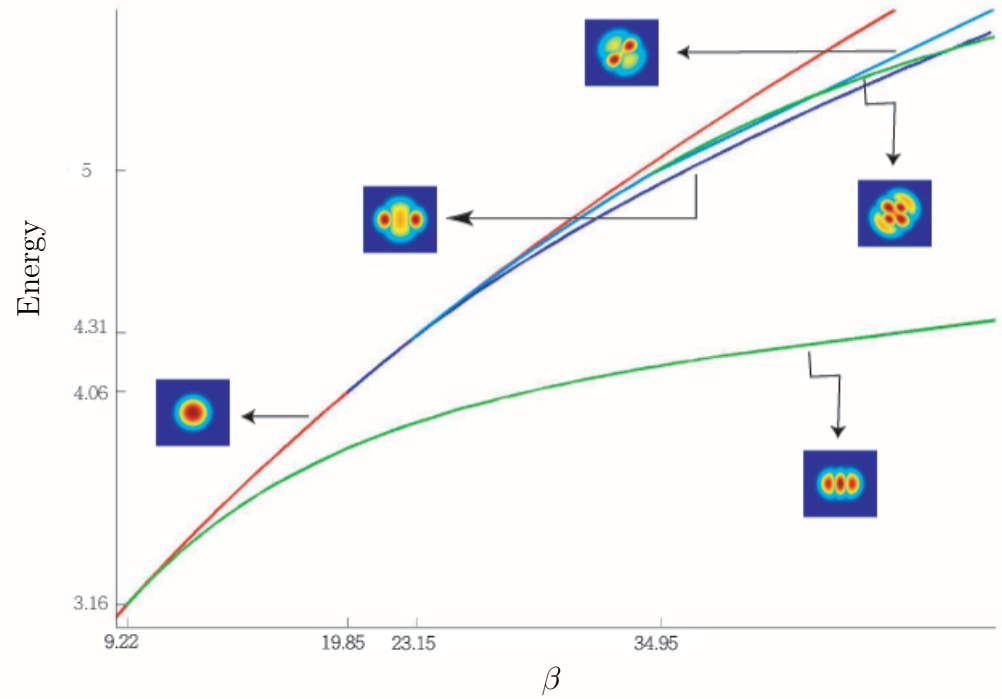

Figure 4.6. $m = 3$. Solution curve of energy versus β for $\beta \in (8.7, 51)$.